AST5-CT-2006-030729

ATLLAS

Aerodynamic and Thermal Load Interactions with Lightweight Advanced Materials for High Speed Flight

SPECIFIC TARGETED RESEARCH PROJECT

Thematic Priority – 1.4
AERONAUTIC and SPACE

Deliverable Reference Number: D.2.4.2
Deliverable Title:

Report on the application of MDO approaches for a Mach 6 SST

Due date of deliverable: 31th of December 2009

Actual submission date: 18th of March 2010

Start date of project: 1st of October 2006

Duration: 39 months

Organisation name of lead contractor for this deliverable: DLR AS-RF (Braunschweig)

Revision #: 0

Project co-funded by the European Commission within the Sixth Framework Programme		
Dissemination Level		
PU	Public	X
PP	Restricted to other programme participants (including the Commission Services)	
RE	Restricted to a group specified by the consortium (including the Commission Services)	
CO	Confidential, only for members of the consortium (including the Commission Services)	

APPROVAL

Title	**issue**	revision
Application of MDO Approaches for a Mach 6 SST	2	0

Author(s)	**date**
Robert Dittrich	31.05.10

Approved by	**date**
J. Longo	
T. Eggers	31.05.10

Table of contents

List of Figures

List of Tables

Nomenclature

Acronyms

BOC	Begin of Cruise
CFD	Computational Fluid Dynamics
COG	Centre Of Gravity
CR	Cruise
DLR	DLR, German Aerospace Center (www.dlr.de)
EOC	End of Cruise
F	Fuel
FEA	Finite Element Analysis
FEM	Finite Element Method
FOI	FOI, Swedish Defence Research Agency (www.foi.se)
GTOW	Gross Take-Off Weight
HS	Horizontal Stabilizer
MDA	Multidisciplinary Analysis
MDO	Multidisciplinary Optimization
OEW	Operating Empty Weight
RANS	Reynolds-Averaged Navier-Stokes
SST	Supersonic Transporter
TS	Transonic

1 Executive summary

1.1 Scope of the deliverable

The deliverable contents the application of the MDO process presented in D2.4.1 ”Report on DLR MDO tool for high-speed design” [3] to the Mach 6 configuration of the ATLLAS project. Hence the presented paper concentrates on the Mach 6 configuration and the aspects of the characteristics and results of the performed MDO runs.

The deliverable describes the HYCAT 1A configuration which serves as the baseline design. Furthermore the used and provided configuration input and assumptions are shown. After the description of the structural modelling the internal structural optimization is presented to determine FEM element properties. Furthermore explanations concerning aerodynamic analyses and propulsion integration are given. After the definition of the design parameters the performed MDO runs are presented. The deliverable continues with a detailed discussion on the characteristics and results of the final 3-point MDO run of the ATLLAS project. Finally a conclusion including general design issues and future work on the MDO process end the report.

1.2 Results

The major results of this work are:

- The functionality of the MDO process is shown
- Cruise range of Mach 6 configuration can be improved significantly
- Structure and propulsion effects are dominating over aerodynamic improvements
- Future possibility of MDO processes is shown

1.3 Specific highlights

Some specific highlights implemented into the MDO process are:

- Successful coupling of CFD, FEM, multiple mission point analysis, propulsion integration and trim capability determination in one multidisciplinary analysis tool
- Process linkage to massive parallel computing system
- Process application on the ATLLAS Mach 6 SST
- Successful demonstration of the functionality and capability of the MDO process
- Cruise range improvement of 38 %
- Major influence due to improvement in structural design and mass ratio
- Improvement in aerodynamic-propulsion interaction performance

1.4 Forms of integration within the workpackage and with other WPs

The MDO process and application relies on specific data of all involved physical disciplines. This data on the one hand defines tool and application requirements and constraints and on the other hand it determines the accuracy of the MDO process. During the project several data was provided by the ATLLAS partners:

- Combustion chamber data provided by DLR-SART (WP2.4.2)
- Initial mission profile provided by DLR-SART (WP2.4.2)
- Initial mass budget based on the HYCAT-1A data provided by DLR-SART (WP2.4.2)
- Initial FEM modelling and analysis procedure provided by FOI (WP2.4.2)
- Geometry engine data (intake and dimensions) provided by ONERA (WP2.4.4)
- C/C-Sic material data provided by WP3 and used for leading edges (WP3.3.2)
- Aluminium alloy material data provided by DLR-SART and used for tank walls (WP2.4.2)

Furthermore data from the presented work was distributed to several ATLLAS partners:

- Initial and optimized geometry sent to several partners
- Aerodynamic data of ATLLAS M6 reference configuration sent to DLR-SART for initial mission analysis (WP2.4.2)
- Aerodynamic data of ATLLAS M6 reference and optimized configuration sent to ONERA for sonic boom analysis (WP2.1.2)
- Nozzle pressure distribution sent to FOI for nozzle structural design (WP5.4.2)

2 Introduction

The presented work covers a newly developed multidisciplinary optimization (MDO) process for the preliminary design of hypersonic configurations. The work is part of work package 2 "*Novel concepts for high-speed flight*" and is integrated in the sub work package 2.4 "*Mach 6 Supersonic transport (SST) configuration*". It is not the aim of this work package to design a specific Mach 6 vehicle but to explore today's state of the art technology limits to realize such kind of concept. The HYCAT 1A configuration [1][2] designed by Lockheed in the late 70's provides the baseline concept for work package 2.4 and hence derived data of the HYCAT 1A is also used in this work which was provided by several ATLLAS partners.

In generally hypersonic configurations are highly complex and integrated systems and characterized by several physical and technical problems e.g. airframe-propulsion integration, propulsion efficiency, low lift to drag ratios, high-speed versus low speed performance and strong sonic boom effects. Frequently one problem is linked to another one. Furthermore real flight data is hardly available; hence validation of design tools like numerical computations is difficult. To consider disciplinary linkages in a hypersonic design process a multidisciplinary treatment is necessary. In addition with numerical tools like CFD and FEM and the usage of massively parallel CPU power the hypersonic design process can be transformed to a multidisciplinary optimization process. Today a multidisciplinary optimization technique could provide the right platform to come closer to the realization of such kind of vehicle as is the aim to demonstrate in the present work.

Due to the objective using numerical tools for the MDO process the DLR TAU code is chosen as aerodynamic flow solver. TAU is a Reynolds-averaged Navier-Stokes flow solver applicable for subsonic as well as hypersonic cases. At the beginning of the work no multidisciplinary framework using the DLR TAU code for a hypersonic MDO process existed. The implementation of a CFD code into a multidisciplinary environment requires further special methods for grid generation and data pre- and post-processing. Hence two major objectives of this work can be defined:

- Development of a new MDO tool for hypersonic applications
- Performing of a MDO process for a given hypersonic application

In this deliverable the focus is laying on the 2nd topic, however the setup and the technical background of the MDO tool is described more precisely in deliverable D2.4.1 [3]. The first point for performing the MDO is the allocation of all input data which is mandatory needed to run the optimization. This includes all data which is not computed during the multidisciplinary analysis (MDA) chain. The input database contains mass, propulsion and mission data and is presented in the corresponding chapters. After all input data is given and the MDO modules adjusted to the ATLLAS Mach 6 application. Furthermore the design parameters which are allowed to change during the optimization process need to be defined. On the one hand as much as possible parameters are favoured, but on the other hand the number of design parameters has a big impact on the overall processing time which is laying in orders of months for the presented MDO process. Due to the chosen SUBPLEX optimizer there is no need to perform additionally sensitive studies for the design parameter which can be also a time consuming process. Finally after an optimization procedure is started the user influence on the process is in generally very low and restarting of the process should be avoided. The major work of the user is the adjustment of the MDO modules concerning the hypersonic configuration.

3 Prerequisites

In the following chapters specific settings, assumptions and helper methods used in the MDO process are summarized. The MDO process itself consists of several modules. Each module covers a closed field of activity e.g. geometry generation or CFD calculations. The several modules and their functions are described in detail in the report of the MDO tool [3]. In the following chapters some important aspects for the application of the MDO tool on the ATLLAS Mach 6 configuration are exposed.

3.1 Reference configuration based on the HYCAT 1A

The HYCAT 1A configuration [1][2] designed by Lockheed in the late 70's provides the baseline concept for work package 2.4 of the ATLLAS project. Derived data of the HYCAT 1A configuration is used in this work which was provided by several ATLLAS partners for several disciplines. The main characteristics of the HYCAT 1A are a 105 m long fuselage, a span width of 30 m, a double elliptic fuselage cross section shape with sharp edges on the forebody and a horizontal tail. Furthermore it was planned to carry about 200 passengers on a 9000 km mission with a cruise Mach number of 6. This would strongly reduce the overall mission time e.g. travelling London to Rio in 90 minutes. The HYCAT 1A has a highly integrated turbo-jet/ram-jet propulsion system driven by hydrogen. The fuselage contains a front and rear hydrogen tank whereas the passenger cabin is residing in the middle. The gross take off weight is 278000 kg. Figure 3.1 shows the setup of the HYCAT 1A configuration of the original reports. The HYCAT 1A data serves as main input for the reference configuration of the MDO process which is shown in Figure 3.2. Before the MDO process several iteration steps with the ATLLAS partners were performed to update the reference configuration. Initial aerodynamic CFD calculations on the reference configuration supported the creation of a reference mission which in turn was used during the MDO process. ATLLAS partner FOI used the reference configuration for the development of the FEM model and the structural design.

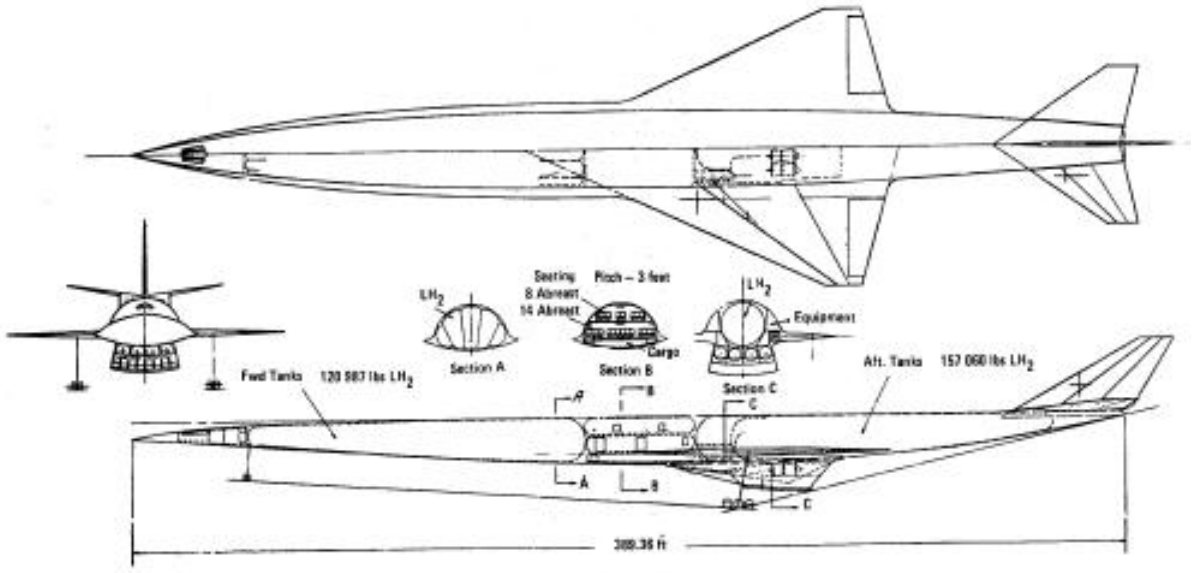

FIGURE 5-14. HYCAT-1A: Mach 6, 200 passenger transport.

Fig. 3.1: HYCAT 1A configuration

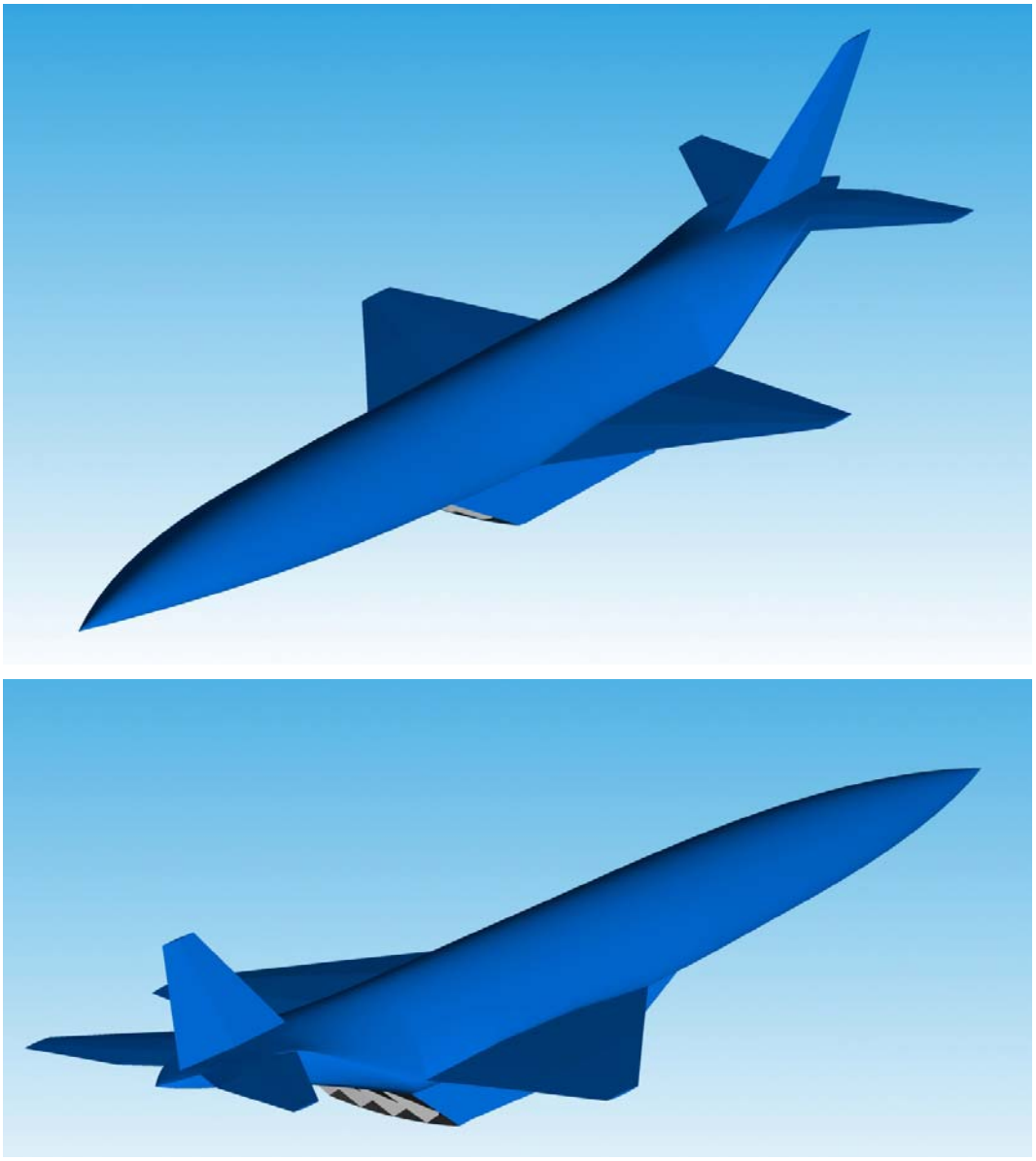

Fig. 3.2: Reference geometry based on HYCAT 1A data

3.2 Mass budget and structural analysis

The initial mass budget in generally is based on the HYCAT 1A data and the details were provided by the ATLLAS partner DLR-SART. The mass data is listed in the Tables 3.1 and 3.2. For the association of mass data in the MDO process there is a principal classification of the mass components into two groups, 1) constant masses and 2) masses depending on the structural layout. In the Tables the constant mass components are highlighted in blue and structural masses are highlighted in yellow. Constant masses represent all subsystems and configuration components which are assumed to be unmodified during the MDO process like gears, furnishing or hydraulics. Hence before the MDO process is started different masses of the mass budget have to be assigned either to be a constant mass or be part of the structural mass which for the HYCAT 1A results in a simplified mass table demonstrated in Table 3.3 on the left side.

Stage # 1	HYCAT-1A ATLLAS -Recalculation supersonic cruise aircraft M= 6		Mass [kg]
1. 1	Structure group:		
1. 1. 1	Hypersonic Vehicle Body (HASA)		34197,98
1. 1. 2	Take-Off Wing Structure		18050,43
1. 1. 3	Fins / Vertical Stabilizer		4547,73
1. 1. 4	Wing Control Flaps		2251,12
1. 1. 5	Tank		12000,00
1. 1. 6	Tank		12000,00
1. 1. 7	Thrustframe A/B-Engines		1019,68
1. 1. 8	Nacelles		1400,00
	Mass Structure group:	w/o margins	85466,95
	Mass Structure group:	including 10.0 % margins	94013,64
1. 2	Subsystem group:		
1. 2. 1	Propellant Supply		580,48
1. 2. 2	Propellant Supply		362,84
1. 2. 3	Take-Off Gear		10800,00
1. 2. 4	Electrics		3086,63
1. 2. 5	Avionics		600,00
1. 2. 6	Hydraulics		2466,62
1. 2. 7	ECS		800,00
1. 2. 8	Primary Power		1500,00
1. 2. 9	Paint		2400,00
1. 2.10	Air-Conditioning		3300,00
1. 2.11	Furnishing		10000,00
1. 2.12	Fairing		0,00
	Mass Subsystem group:	w/o margins	35896,56
	Mass Subsystem group:	including 10.0 % margins	39486,22
1. 3	Propulsion group:		
1. 3. 1	Airbreathing Engines Turbo		12500,00
1. 3. 2	Airbreathing Engines (SC)RAM		6000,00
1. 3. 3	Air Intake		8000,00
1. 3. 4	Airbreathing Engines Nozzle		10000,00
	Mass Propulsion group:	w/o margins	36500,00
	Mass Propulsion group:	including 10.0 % margins	40150,00
1. 4	Thermalprotection group:		
1. 4. 1	TPS #2		3081,50
1. 4. 2	Cryogenic Insulation		1408,00
1. 4. 3	Cryogenic Insulation		1474,00
	Mass Thermalprotection group:w/o margins		5963,50
	Mass Thermalprotection group:including 10.0 % margins		6559,85
	Stage Mass empty: (stage coordinates)		163827,01
	Stage Mass empty incl.marg.: (global coordinates)		180209,71
	Residual propellant:		1000,00
	Reserve propellant:		1000,00
	Stage Mass @ burn out (fairing separated):		182209,71
	Payload Mass:		18990,29
	Ascent propellant:		97050,00
	GLOW Stage Mass (w/o payload):		279259,71

Table 3.1: Initial mass budget – Part 1

HYCAT-1A ATLLAS -Recalculation		
Total Vehicle Mass empty:	163827,01	
Vehicle Mass empty incl. margins:	180209,71	
Total Lift-off Mass:	279259,71	
Payload Mass of stage 1 :	18990,29	
Gross Lift-Off Mass:	298250,00	
* = user provided mass input		
** = stsm supercomponent data set		
	DLR-SART	Lockheed (Brewer)
Vehicle Mass empty incl. margins:	180209,71	162070,00
Ascent propellant:	97050,00	97020,00
Payload Mass:	18990,29	19050,00
Gross Lift-Off Mass:	298250,00	278140,00

Table 3.2: Initial mass budget – Part 2

HYCAT 1A	
constant	
payload	18990,29
subsystems	31060,06
gears	10800,00
engines	18500,00
sum	79350,35
stucture	
airframe structure	85466,95
engine structure	18000,00
sum	103466,95

ATLLAS M6 SST	
fem - constant	
payload	19000,00
subsystems	36000,00
gear_bow	3300,00
gear_main (2)	9000,00
engines	18500,00
sum	85800,00
% relative	8,13
fem - structure (initial opt.)	
fuselage	42518,00
tank_bow	2933,00
tank_rear	4364,00
wing	11210,00
hori. stab.	5923,00
vert. stab.	2185,00
engine	17300,00
sum	86433,00
% relative	-16,46

Table 3.3: Mass budget divided in constant and structural masses

After this principal classification the following main objectives of the mass and structure analysis can be defined:

- Determination of preliminary structural layout and structural masses
- Determination of maximum fuel mass
- Determination of a centre of gravity (COG) range depending on different fuel levels

These objectives have to be solved for every configuration during the MDO process. To reach these objectives the numerical method of finite elements (FEM) is used to increase result accuracy. During the ATLLAS project the partner FOI designed an initial FEM model composed of shell and bar elements describing the basic structural layout. Furthermore element properties, material types and material groups were given by the FOI model. The FOI model was adapted and modified to the MDO process which includes a PYTHON controlled mesh generation procedure.

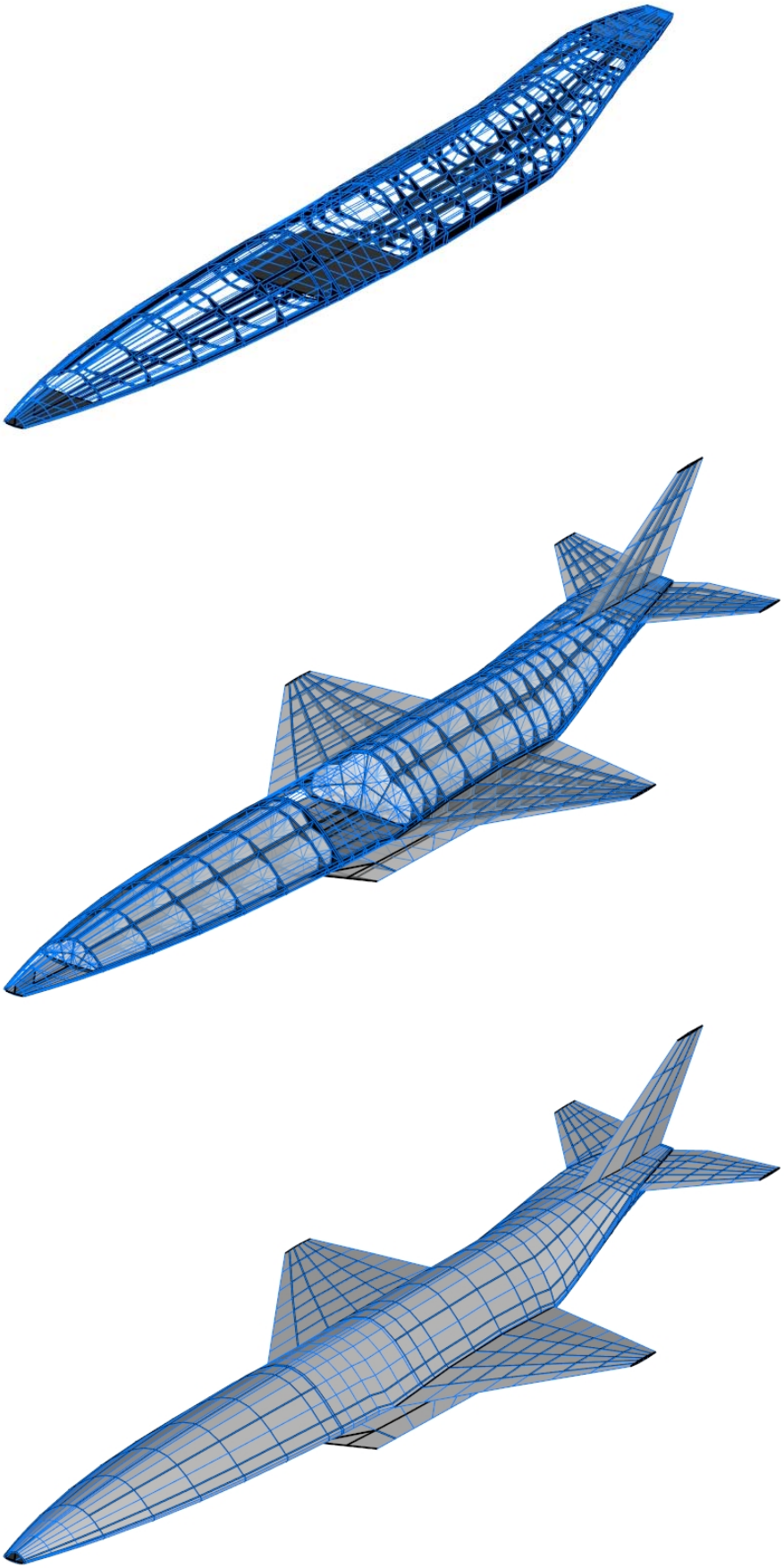

Fig. 3.3: FEM model states

The mesh generation procedure is based on the geometry generation procedure which was also developed during the ATLLAS project, see also [3]. Different states of the mesh procedure are shown in Figure 3.3. Depending on a given outer geometry a FEM model based on the FOI strategy is generated in NASTRAN specific format. Therefore the several configuration geometry parts like the fuselage, the engine and the wings are cut at certain positions, so nodes describing frame stations respectively cross sections are generated. By connecting these nodes with shell elements the configuration covers for fuselage, engine and wings are created. Afterwards the several parts are connected via so called rigid body elements to form fix structural interfaces between several configuration parts. After the outer shells are created the mesh procedure continues by building the inner parts of the configuration. To simulate wing ribs and spars shell elements are used for both, connecting nodes in span width direction and filling the wing cross sections. The inner engine model is very simplified by including simple straight walls for intake and nozzle walls. The propulsion units of the turbojet and ramjet are added later using concentrated mass elements. Against that for the inner part of the fuselage the detail is increased. The fuselage is mainly characterized by the bow and rear tank as well as the passenger cabin. Furthermore there are small parts at the very beginning and ending of the fuselage for additionally space. Every frame station can be assigned to one of these inner fuselage design types. DLR-SART has developed a multi-loop tank design during the ATLLAS project. A simplified approximation to consider the multi-loop tank design approach is considered for the tank frame stations in the FEM mesh generation procedure. For every frame station next to the outer knot profile an inner knot profile is created. Both profiles are then connected with shell elements. To improve stiffness bar elements with I-shaped cross sections are introduced in radial and axial direction of the fuselage. A final tank frame station is shown in Figure 3.5. In the next step of the mesh procedure all inner walls of the fuselage are generated. This includes bottom walls at front, end and cabin stations as well as tank walls and vertical walls near the fuselage sides. The vertical walls were already introduced by FOI because initial eigenvalue analyses have shown poor stiffness characteristics especially at the sharp edged fore body. This was improved a lot by including the additional vertical walls. Like all inner walls the tank walls are also built by shell elements. Each of the both tanks is described again by an outer cover and inner walls. Similar to the outer fuselage cover the tank cover is created by the connection of the inner node profiles of the tank frame stations. Hence the inner knot profiles are simultaneously the interfaces between tank and fuselage. The last step of the FEM node and element creation is the distribution of 1-dimensional elements, so called concentrated mass elements. These elements can be coupled to a certain node and later charged with a mass value.

Until here the whole MDO FEM modelling procedure needs no special input values and can be built by only giving the outer geometry. At this stage the model consists of about 10000 elements. But as mentioned the element properties are still not defined. But before defining element properties the used materials are specified. Materials are given by the FOI model. Used materials are steel, aluminium, aluminium alloy and an aluminium-beryllium-alloy also known as Lockalloy or AlBeMet which is almost as stiff as steel but has a significantly lower density. FOI replaces some parts of the fuselage cover by AlBeMet which seriously improves the dynamic behaviour of the configuration [4]. However the high costs of AlBeMet have to be mentioned which are not considered in the MDO process at the moment. The material properties were provided by FOI and transformed to the MDO material library which is was slightly extended by the C/C-SiC material for leading edges claimed by high temperatures. The material properties for C/C-SiC were provided by work package 3 [7] of the ATLLAS project and integrated to the structural process as anisotropic material, see Table 3.4. The arrangement of the several material groups is shown in Figure 3.4.

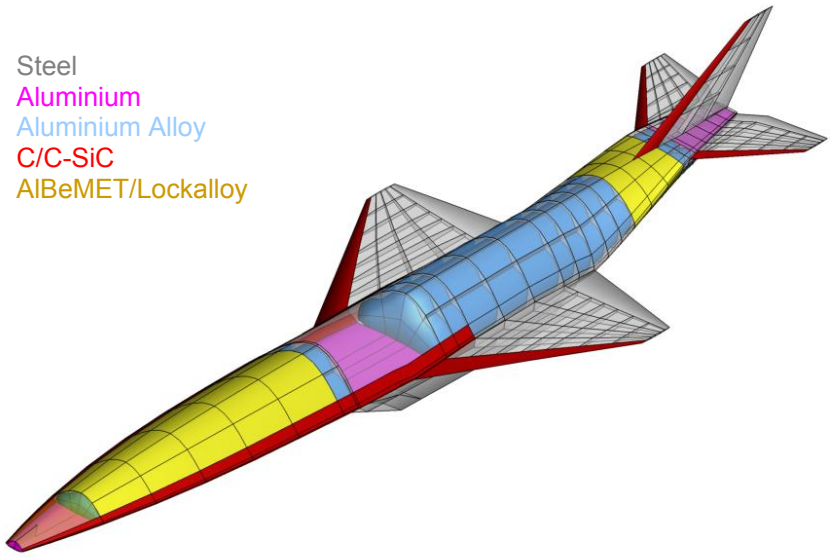

Fig. 3.4: FEM material groups

Material	E [GPa]	G [GPa]	Nue	Rho [kg/m³]
Steel	210.0	80.8	0.30	7600
Aluminium	70.0	26.3	0.30	2700
Aluminium Alloy	75.0	28.0	0.33	2700
AlBeMet	200.0	76.9	0.30	2076

Material	E1 [GPa]	E2 [GPa]	Nue12	G12 [GPa]	Rho [kg/m³]
C/C-SiC	74.1	25.8	0.0316	8.8	1850

E Young's modulus
G Shear modulus
Nue Poisson's ratio
Rho Density
i Material direction

Table 3.4: Material data

In the next step the constant masses, according the mass budget given at the beginning of the chapter, are considered in form of concentrated mass elements which are applied to the FEM nodes. Four constant mass groups can be defined: subsystems, payload, engines and gears. The engine and gear positions are inherited of the HYCAT 1A reference. The masses are not distributed as a single mass but disposed on surrounding nodes of these positions. The payload mass is distributed along the bottom wall of the cabin frame stations. Finally the mass of the subsystems is distributed along the whole fuselage by calculating the mass per meter of the configuration length which assumes a smooth distribution of the subsystems along the axial direction. Hence depending on the number and position of the simulated fuselage frame stations the single mass for every frame station can be determined. Against that the distribution at a single frame station is not smooth but the mass is concentrated in free geometrical space which is given by the presented multi-loop tank design. This is demonstrated in Figure 3.5. In the Figure the numbers describe the percent of frame station mass connected to the corresponding node.

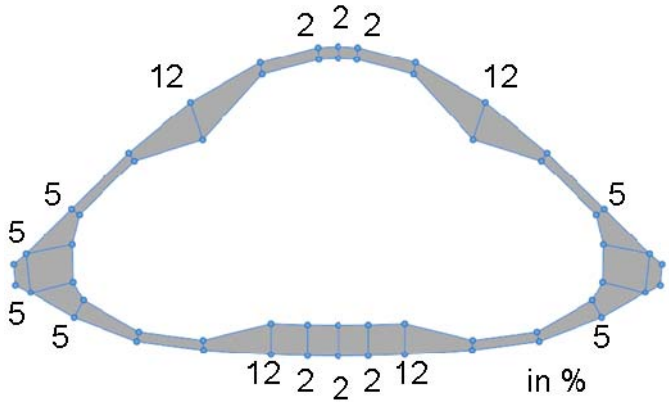

Fig. 3.5: Distribution of a given mass at a frame station (in %)

At this modelling stage the only missing mass is the fuel mass. There are two different aspects concerning the fuel mass. First, the maximum fuel mass is determined by calculating the tank volumes. This is done by building 3-sided prisms between the tank frame stations to consider the multi-loop tank design. The maximum fuel mass is then determined by 85% of these volumes and the density of hydrogen of 75.98 kg/m³. The second aspect is the determination of the centre of gravity depending on the fuel level. Therefore a given fuel mass is distributed on the inner frame station nodes similar to other constant masses which means that again concentrated mass elements are used. For every given fuel mass between empty and maximum fuel two kinds of distribution are performed. In the first mode as much as possible mass is distributed into the bow tank and if there is any, the rest is put into the rear tank. The second mode is the opposite; hence it is starting with the rear tank, see also right part of Figure 3.6. With this approach a maximum and minimum centre of gravity is determined. All values in between are feasible due to the emptying of tanks can be directly controlled. Hence for every configuration a range of centre of gravity depending for every fuel level can be determined. If later the centre of pressure is residing within this range it is assumed the configuration can be trimmed. These are important constraints at the covered mission points during the MDO process. As example the range of the centre of gravity of the initial configuration at begin of cruise conditions is 7 m which is 6.6 % of the configuration length.

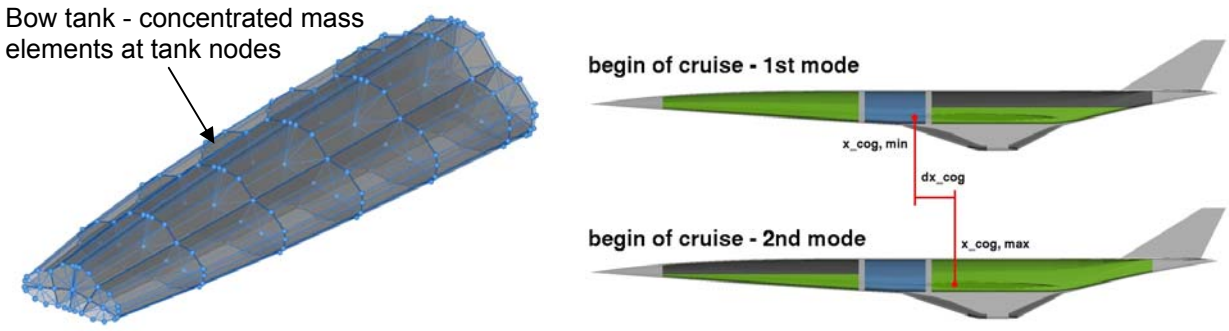

Fig. 3.6: COG determination, left) FEM bow tank model with concentrated mass elements, right) possible modes of tank emptying and COG shift

The definition of the element properties is not a trivial task. For example simple shell elements have a thickness parameter and I-shaped bar elements have 6 parameters. Thus defining every single element property independently is not a good choice. To reduce the number of property parameters FOI created a property group system in their initial model. Every group represents a bigger structural part and contains a set of elements. Changing the group properties changes

element properties accordingly. At the moment groups are restricted to one element and one material type. In general groups of the fuselage are divided in axial and circumference direction and groups of wing elements are divided in span width and chord direction. The approach of the property group system of FOI is transferred to the MDO FEM procedure. Finally the group system contains 108 groups with 199 structural parameters. FOI analysed the group properties of their model in an iteration process by manually changing different parameters. In the MDO process this method is automated by using the NASTRAN internal optimization capabilities. The FOI group properties serve as default values after the model generation and before the optimization. The final property values are then determined by the gradient based optimization method of the NASTRAN solver. If the structural optimization fails at any reason the MDA chain continues using the default masses as fallback. The overall MDO loop time is increased by applying a structural optimization process, but structural design can now directly react on geometry changes. Without using parallel computations the complete FEM procedure takes about 30 minutes whereas 95 % of the time is needed for the structural optimization. The latter is running once per global MDO iteration. Against that the determination of the centre of gravity depending on fuel mass is fast and can be repeated several times per iteration for different cases.

A reasonable structural optimization needs the definition of an objective function and suitable constraints. For the structural optimization process minimum element property values have to be declared which are a minimum thickness of 0.8 mm for shell elements and 1.0 mm for bar cross section parameters. The objective function is the minimization of the structural weight. To avoid that the structural optimization would simply lead to the minimum declared element properties two different constraints are defined. First, a minimum frequency of 2.5 Hz has to be achieved for the first mode of a free eigenvalue analysis. This is performed by using NASTRANs “normal modes” solver without further constraints. Here the maximum fuel mass is applied to the structural model forming the worst case. Second, a pressure load case is applied on the wings and the horizontal stabilizer checking for the maximum “von Mises” stresses. In a first approach for the maximum allowed “von Mises” stress 400 MPa is chosen. To decrease this value the effort on FEM modelling and analyses have to be increased to find feasible solutions. On the other hand the value is in the limit range of some of the used materials. However this issue is identified as an important point for improvement in the future. The pressure distributions of several cruise configurations of the first MDO process of the ATLLAS project were analysed. Due to the double trapezium wing profiles the pressure distribution can be divided to specific surface segments of the wings. Comparing these surface segments shows that the pressure differences of several wings in Mach 6 cruise conditions are relatively low so that forces respectively bending moments are mainly driven by the wing geometry. So every wing is loaded with the same pressure distribution and the stresses are calculated. The pressure distribution is multiplied by a load factor of 2.5 which can be compared to a cruise pull-up manoeuvre. The idea behind this stress load case is that there is no mass loss at the fuselage wing interfaces and the wings itself by considering only a dynamic constraint. For the same reason there are no structural parameters at the outer sections of the wings. Also it has to be mentioned that this is a first approach to include a static load case into the structural optimization which was not originally planned. The main focus was concentrated to the dynamic analyses. The structural constraints are checked twice, within the internal NASTRAN optimizer and in the MDO objective function update module.

Using the presented approach the structural and fuel masses are determined for every configuration in the MDO loop. For the initial configuration the result is shown on the right side of Table 3.3. In the constant mass fraction a margin of 8%, similar to the initial mass budget, is considered. The structural mass is reduced by 16% against the HYCAT 1A structural mass. One of the main impact is the lower tank masses which were estimated very high in the original design.

3.3 Performance of aerodynamic analyses

The numeric flow calculations are performed using the DLR TAU code [5], a Reynolds-averaged Navier-Stokes (RANS) flow solver applicable for subsonic as well as hypersonic cases. For reducing flow solver time TAU is running in Euler mode in addition with large parallel computing. Fast convergence is reached using three level multigrid, 2nd order AUSMDV upwind scheme for flux discretization and the three step Runge-Kutta method for relaxation solving. The targeted lift is provided as input hence the resulting angle of attack and flow field is numerically computed. The TAU code is running on the DLR CASE cluster consisting of more than 5000 CPUs whereas 80 CPUs are used for each CFD calculation. The needed CPU time for a cruise CFD calculation using grids with about 1.5 million nodes is below 8 minutes. The CFD computations are controlled via PYTHON scripts which overtake all sub tasks e.g. network communication, data transfer, solution checks and data monitoring. By using PYTHON threading capabilities several independent aerodynamic cases can be calculated in parallel which leads to further loop time reduction.

Due to the numeric solving of the Euler equations an additional skin friction model is added to consider viscid effects. The missing skin friction is implemented to the force calculations after the CFD. Therefore the method of a turbulent flow around a flat plate is assumed. The skin friction coefficient can be described by:

$$c_{sf} = 0.455\left(\frac{T_w}{T_\infty}\right)^{-1} \log\left[\left(\mathrm{Re}\left(\frac{T_w}{T_\infty}\right)^{-2.8}\right)^{-2.58}\right] \tag{3.1}$$

With the Reynolds number Re formed by current mission point conditions and configuration length. The temperature ratio is depending on the Mach number:

$$\frac{T_w}{T_\infty} = 1 + 0.45(\kappa - 1)M^2 \tag{3.2}$$

The drag coefficient $C_{d,sf}$ due to skin friction is:

$$C_{d,sf} = c_{sf}\,\frac{A_{wet}}{A_{ref}} \tag{3.3}$$

A_{wet} is the complete wetted surface area of the configuration and A_{ref} is the reference surface area defined as the top view projection surface area of the entire configuration. Both surface areas are determined within the geometry generation process. The skin friction coefficient is then added to the drag coefficient of the Euler CFD calculation.

$$C_d = C_{d,euler} + C_{d,sf} \tag{3.4}$$

In the work of a diploma thesis [6] at DLR-RF the viscid influence on a simplified ATLLAS Mach 6 model was investigated. Table 3.5 shows the drag coefficient for different solver cases including

laminar and turbulent calculations and the presented skin friction model approach. In the original flat plate version it is shown that the skin friction is between the laminar and turbulent case. By including a factor into equation 3.1 leads to:

$$c_{sf,ext} = k \cdot c_{sf} \tag{3.5}$$

By changing factor k the final drag coefficient can be shifted between full laminar or full turbulent conditions. In the presented work factor k is set to 1.5 which matches the turbulent conditions.

Solver case	Drag coefficient
RANS, laminar	6.99E-03
RANS, turbulent	8.51E-03
EULER	6.28E-03
EULER + skin friction model, k = 1.0	7.78E-03
EULER + skin friction model, k = 1.5	8.53E-03

Table 3.5: Drag coefficient depending on solver case

3.4 Propulsion integration

One of the major aspects of the MDO process is the consideration of the integrated propulsion system. This includes the acquisition of the propulsion influence to the configuration performance which poses a challenge in modelling and analysis due to the propulsion system influences almost all modules of the MDO process. The modelling and analysis of propulsion systems is not a trivial task especially in iterative design processes, hence some simplifications and assumptions have to be introduced into the MDO process.

The engine consists of combined turbo-jet/ram-jet propulsion system and is driven by hydrogen. For the modelling approach in the MDO process a so called “black box” engine model is used. There are four parallel engine channels. Every channel is characterized by a three ramp intake, the “black box” and the nozzle. The “black box” is a simplified element to describe the inner components of the engine e.g. diffuser channel and combustion chamber. The intake and the nozzle geometry and their flow field are directly considered in the MDO process. Against that “black box” components are not modelled, but they are considered as CFD input and boundary conditions, in the force balance and the mass budget.

The engine geometry was initially adapted by the HYCAT 1A design and later in the ATLLAS project it was updated and specified by the ATLLAS partner ONERA which includes a CAD file describing the outer engine dimension and the three ramp intake. The CAD geometry is transformed to the MDO geometry generation procedure. Hence the engine geometry is also parameterized and described by 40 parameters. However the most parts of the engine geometry is unchanged during the MDO. At the moment only the nozzle geometry is variable by considering four nozzle parameters in the design parameter set. Taking also the intake geometry into account generates several new design parameters as well as MDO complexity and computational costs increase rapidly. This is the reason why two different MDO processes were targeted within the ATLLAS project. The MDO process led by ONERA was concentrated on the intake design while the presented MDO process is focused on the airframe.

Fig. 3.7: View on engine intake

The propulsion flow data was provided by ATLLAS partner DLR-SART [8]. The data contains the flow conditions for the combustion chamber inflow and the nozzle throat area for three different Mach numbers. For Mach number 1.3 and 6.0 the flow conditions are listed in the Tables 3.6 and 3.7 like they were used during the MDO. For every Mach number the flow parameters are given for different throttle levels and intake losses. In the MDO process $\eta = 0.95$ is used. Linear interpolation is applied to determine parameters for throttle levels which are not listed in the Tables. On the one hand the values are then used for the boundary conditions during the CFD calculations. On the other hand the propulsion data allows the determination of the combustion chamber gross thrust using the equations of momentum. These forces are needed to complete the force budget of the configuration.

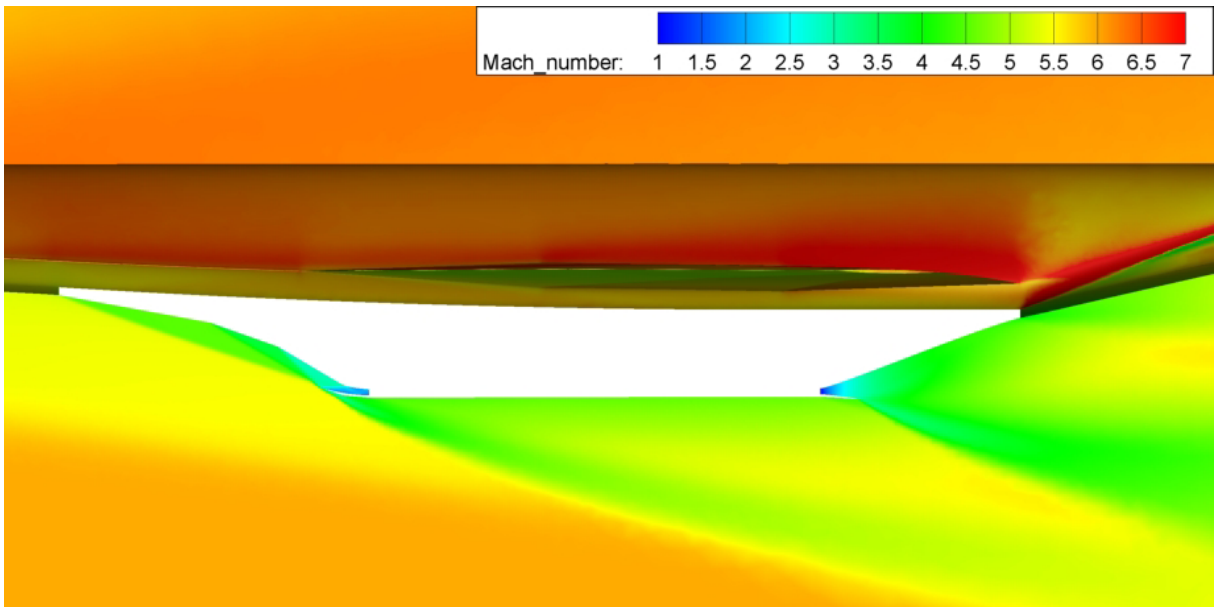

Fig. 3.8: "Black box" engine model – CFD intake and nozzle flow in cruise conditions

Due to the chosen engine model intake and nozzle flow have to be considered in the CFD module of the MDO process. The main objective of the CFD is the calculation of the pressure signature on the wall to determine the forces and force depending data in a global view of every configuration. Hence simplifications and assumptions are applied in the CFD model.

The intake CFD domain ends at the combustion chamber inlet. After the CFD a PYTHON routine summarizes the flow data at this domain outflow area and compares the data with the combustion chamber inflow conditions of the propulsion data sheet. Occurring differences are handled by a correction force; see the force calculation procedure in [3]. The nozzle domain starts in the nozzle throat assuming a Mach number of 1. Nozzle pressure is given by the propulsion data sheet and applied as boundary condition. As for the whole CFD domain air with perfect gas assumption is used. In the following force calculation the nozzle force is always reduced by 5% due to possible impreciseness of this modelling approach. Figure 3.8 shows a slice trough the engine of a Mach 6 CFD result. It includes the intake shock system as well as the nozzle expansion starting at nozzle throat. Furthermore the flow is characterized of strong shocks on the intake lip and the nozzle.

For the acceleration phase at Mach number 1.3 it is assumed the engine is running at 100% throttle. In all cruise cases the throttle level respectively the fuel mass flow for steady horizontal flight is unique for every configuration. Hence to respect the Breguet range conditions of weight is lift and thrust is drag an interpolation routine is applied to the MDO process. The first condition can be fulfilled by giving the targeted lift as input parameter to the flow solver which is resulting in a corresponding angle of attack. For the second condition more effort is needed. Two CFD calculation with throttle levels of 60% and 80% are performed whereas both in generally will violate the thrust is drag condition. But with two results it is possible to interpolate to thrust minus drag is zero. Afterwards also all forces and force coefficients are interpolated.

For the detailed description of the boundary condition usage, force calculation and further information reference [3] is advised.

M=1.3	alt= 7100 m												
	0,7												
	1			P [Pa]		T [K]		cp [J/kgK]	γ [-]	massflow [kg/s]	fuel-air-ratio [-]	throat area [m**2]	
T_AB= 2650K	eta_intake= 0.985	In	109303,80	78809,62	323,67	294,82	1006,09	1,3994	295,39482	0,00000	-		
		Out	470485,15	268846,70	2650,00	2448,34	2455,86	1,1647	304,69373	0,03148	0,95300		
T_AB= 2400K	eta_intake= 0.985	In	109303,80	78809,62	323,67	294,82	1006,09	1,3994	295,39482	0,00000	-		
		Out	470763,11	266167,39	2400,00	2186,52	2056,57	1,1953	302,95191	0,02558	0,88000		
T_AB= 2000K	eta_intake= 0.985	In	109303,80	78809,62	323,67	294,82	1006,09	1,3994	295,39482	0,00000	-		
		Out	471461,59	261988,00	2000,00	1781,00	1630,87	1,2459	300,81583	0,01835	0,77300		
T_AB= 2650K	eta_intake= 0.97	In	107396,50	77434,43	323,67	294,82	1006,09	1,3994	294,66283	0,00000	-		
		Out	462291,52	264191,46	2650,00	2448,67	2459,79	1,1644	303,94336	0,03150	0,96700		
T_AB= 2000K	eta_intake= 0.97	In	107396,50	77434,43	323,67	294,82	1006,09	1,3994	294,66283	0,00000	-		
		Out	463244,75	257428,39	2000,00	1781,06	1631,26	1,2459	300,07053	0,01835	0,78500		
T_AB= -	eta_intake= 0.97	In	107396,51		323,67		1006,09	1,3994	294,66283	0,00000	-		
		Out	485407,86		1583,29		1448,01	1,2719	298,24145	0,01214	0,65300		
T_AB= 2500K	eta_intake= 0.97	In	107396,50		323,67		1006,09	1,3994	84,20184	0,00000	-		
		Out	98263,61		2500,00		2434,67	1,1705	86,99978	0,03323	1,38200		

Table 3.6: Transonic propulsion data

M= 6.0	alt= 27300 m													
	0,7													
	1													
T_AB	eta_intake			P [Pa]	T [K]		cp [J/kgK]	γ [-]		massflow [kg/s]	fuel-air-ratio [-]	throat area [m^2]
2800	0,9675	In	2036826,91	1486762,32	1583,42	1462,58	1138,57	1,3372		411,58468	0,00000	-
		Out	1854875,64	1043487,83	2800,00	2534,11	2009,72	1,2099		424,13088	0,03048	0,34000
							51,00					
2125	0,9675	In	2036826,91	1486762,32	1583,42	1462,58	1138,57	1,3372		419,35898	0,00000	-
		Out	1863449,74	1036576,32	2125,00	1894,89	1600,53	1,2429		424,46247	0,01217	0,27900
	0,963	In	1886955,32	1377364,99	1583,42	1462,58	1138,57	1,34		411,57205	0,00000	
		Out	1718455,48	966962,20	2800,00	2535,09	2016,95	1,21		424,13011	0,03051	0,37523
		In	1886955,32	1377364,99	1583,42	1462,58	1138,57	1,34		419,23488	0,00000	
		Out	1726265,98	960454,02	2135,58	1905,12	1608,36	1,24		424,45719	0,01246	0,30939
2800	0,95	In	1453992,95	1061328,25	1583,42	1462,58	1138,57	1,3372		411,53555	0,00000	-
		Out	1324352,81	745888,15	2800,00	2537,94	2037,85	1,2065		424,12788	0,03060	0,47700
2166,14		In	1453992,95	1061328,25	1583,42	1462,58	1138,57	1,3372		418,87635	0,00000	
		Out	1329957,37	740545,17	2166,14	1934,66	1630,99	1,2400		424,44194	0,01331	0,39718
2125	0,95	In	1453992,95	1061328,25	1583,42	1462,58	1138,57	1,3372		419,35275	0,00000	-
		Out	1330321,08	740198,43	2125,00	1895,51	1604,58	1,2421		424,46232	0,01218	0,39200
T_AB= 2800K	0,93	In	1021426,22	745580,30	1583,42	1462,58	1138,57	1,3372		411,49291	0,00000	-
		Out	930497,65	524510,37	2800,00	2540,78	2059,44	1,2040		424,12526	0,03070	0,68000
T_AB= 2125K	0,93	In	1021426,22	745580,30	1583,42	1462,58	1138,57	1,3372		419,34812	0,00000	-
		Out	934613,59	520119,58	2125,00	1895,97	1607,58	1,2416		424,46221	0,01220	0,55800

Table 3.7: Cruise propulsion data

3.5 Correlation of MDA chain and flight mission

Figure 3.9 shows the MDO process which was developed during the ATLLAS project. It couples a multidisciplinary analyses (MDA) tool with external optimizer tools. The main work was performed within the white box of the Figure including automated processes for geometry, CFD and FEM grid generation as well as CFD and FEM analyses and general routines for force, mission and post-processing methods. The MDA tool has a modular setup and the computed data of the modules is stored in a global database. The MDO process works with two different optimizers. The first one is for the structural design process which is repeated in every loop. It's a gradient based optimizer included in the NASTRAN package. The second one is the outer main optimizer controlled by the commercial tool SYNAPS POINTER PRO. A function comparison method is used, the so called SUBPLEX optimizer which is often recommended as best optimizer for noisy objective functions. The theoretical background of SUBPLEX optimizer is described in detail in [3].

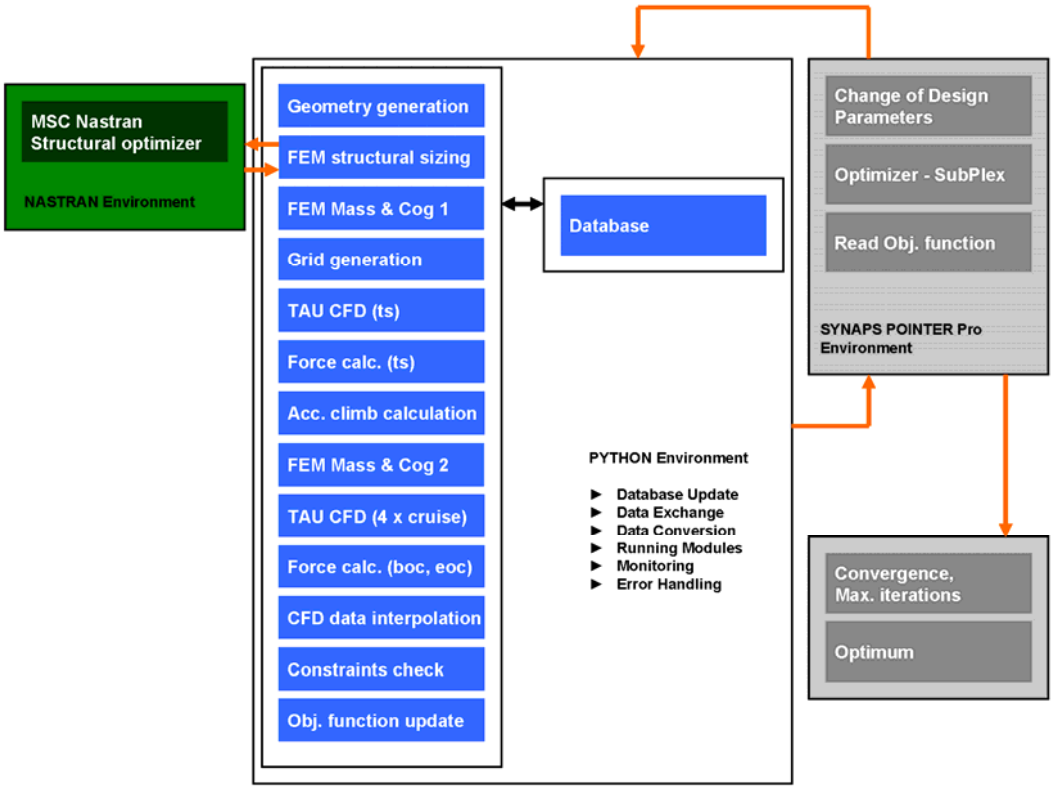

Fig. 3.9: Final MDO process

As already mentioned the core of the process is the MDA tool. Figure 3.10 demonstrates the technical workflow of the MDA tool in an alternative form of 10 major steps. Based on certain input data and the use of one of the major MDA modules described in [3] every step produces an output which is either needed by subsequent steps or fills the database of the current investigated configuration. The right part of Figure 3.10 shows the same MDA workflow by means of a simplified mission profile. The covered mission points are:

- Take off
- Transonic point, H = 7000m, M = 1.3
- Begin of cruise, H = 27300, M = 6.0
- End of cruise, H = 27300+dH_{cr}, M = 6.0, dH_{cr} calculated during analyses

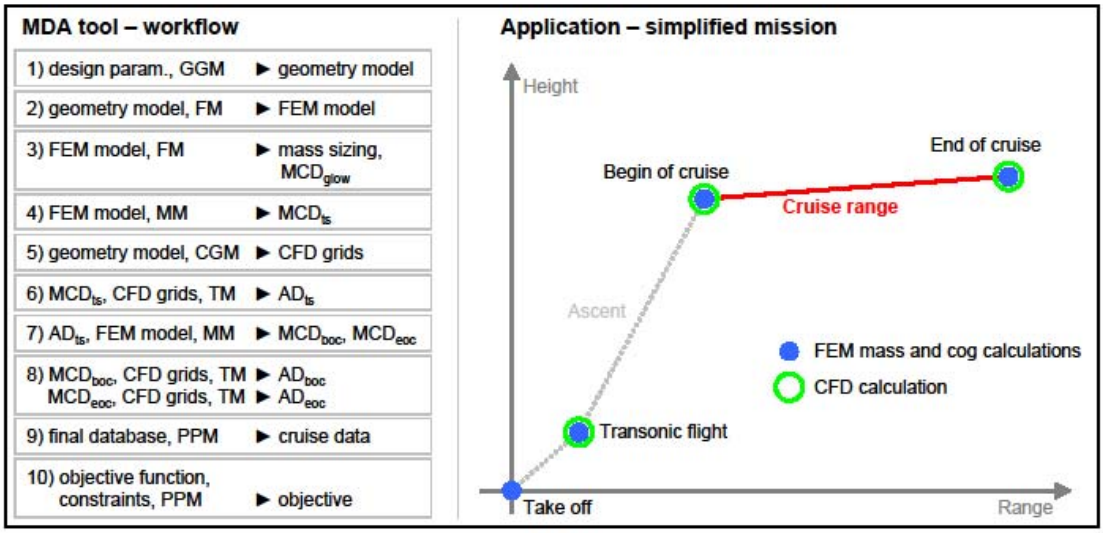

GGM	- Geometry generation module	MCD	- Mass and cog data
FM	- FEM module	AD	- Aerodynamic data
MM	- Mission module	ts	- Transonic point
CGM	- CENTAUR grid generation module	boc	- Begin of cruise point
TM	- TAU module	eoc	- End of cruise point
PPM	- Postprocessing module		

Fig. 3.10: MDA workflow and assigned mission

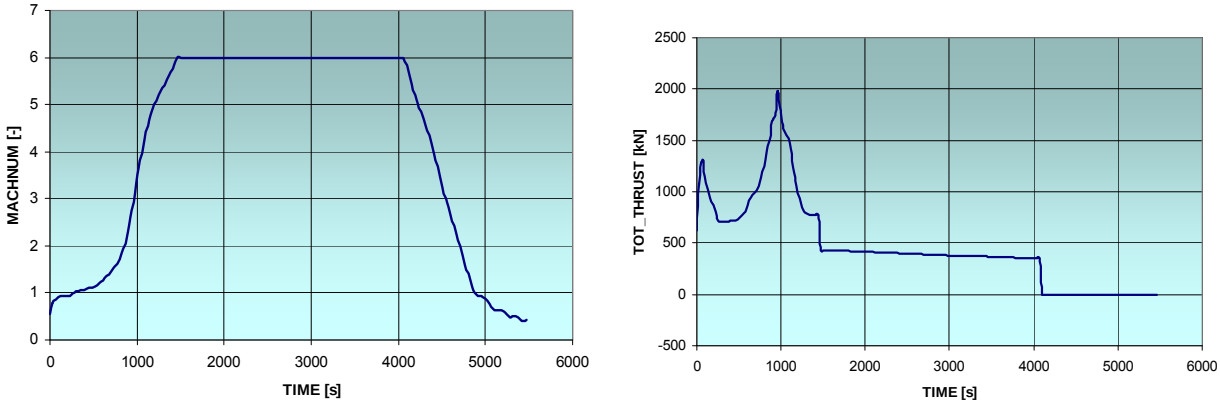

Fig. 3.11: Initial mission data, Mach number and total thrust over time (given by DLR-SART)

The simplified mission profile is deviated by a detailed mission analysis of the reference configuration which was performed and provided by DLR-SART. The mission analysis was supported by this work by several CFD calculations at the beginning of the ATLLAS project. The reference mission data covers the entire flight mission from take of to landing. The mission data is given depending on the time. Figure 3.11 shows as example the Mach number and total thrust characterization of the flight mission. Because not all mission data can be determined during the MDA process at certain points access to the reference mission is needed.

The MDA chain is always starting by the geometry generation depending on a given design parameter set. Afterwards intermediate steps for FEM and CFD grid generation can be performed. With the geometry and the structural layout the final structural element properties are determined by the optimization strategy described in section 3.2. Afterwards the operating empty weight (OEW), the tank volumes, the maximum fuel masses and the gross take of weight (GTOW) are available. The transonic configuration mass is based on the initial mission trajectory resulting in a

fuel reduction of 5% of GTOW to reach the transonic mission point (TS) and based on that the centre of gravity (COG) range for the transonic point is calculated using the FEM model and the transonic fuel mass.

$$m_{fuel,ts} = m_{fuel,\mathbf{max}} - 0.05 \cdot m_{gtow} \tag{3.6}$$

$$m_{ts} = m_{oe} + m_{fuel,ts} \tag{3.7}$$

After the transonic point the mission profile is characterized by an accelerated climb phase until reaching cruise flight at Mach 6. During this phase about 35 % of the fuel is consumed. Together with the fuel consumption after take off almost the half of the fuel is already needed. For this reason the accelerated climb performance on the overall configuration performance have to be considered. But on the other hand acceleration, climbing and mass reduction make an analytical investigation impossible. Hence a simplified climb model was developed during this work and applied to the MDO process. The objective of the climb model is the determination of the consumed fuel mass during the ascent and finally the begin of cruise (BOC) mass. The latter is needed in the objective function. Figure 3.12 shows the fuel consumption for the initial mission profile which is characterized by a strong peak in the middle of the phase. The fuel mass for ascent is defined by:

$$m_{fuel,asc} = \int \dot{m}_{asc} \cdot dt \tag{3.8}$$

In a first approach the climb model reduces the ascent to three points marked as 0,1 and 2 in the Figure 3.12. Further assumptions are:

1) $\dot{m}_{f,ts,100} = const.$
2) $t_{asc} = const.$
3) $\dot{m}_{f,boc} = \dot{m}_{f,asc,2} \approx const.$

This means the fuel mass flow for 100 % throttle in transonic conditions is equal for every configuration. Furthermore it is assumed that the ascent time is constant and the BOC fuel mass flow is constant at 31 kg/s. Hence only points 0 and 1 are unknown and are determined by:

$$\dot{m}_{f,asc,curr,0} = \dot{m}_{f,ts,100} \cdot \frac{D_{ts,curr}}{T_{ts,d,curr}} \tag{3.9}$$

$$\dot{m}_{f,asc,curr,1} = 2.0 \cdot \dot{m}_{f,asc,curr,0} \tag{3.10}$$

Thus one transonic CFD calculation simulating the 100 % case is needed. The targeted lift is given by the mass and the flight altitude of 7000 m. The transonic thrust is defined by the force of the combustion chamber and the magnitude of the thrust is always constant at 1100 kN. Furthermore the combustion chamber thrust is pointing along the configuration axis. Due to geometric design and the targeted lift the angle of attack is altered and influences the “drag” component of the thrust vector which is needed in equation 3.9. But the main influence is due to the transonic drag which is the main idea behind this simplified approach. By increasing transonic drag the fuel mass flow also

increases and less fuel mass is left for the cruise flight. Point 1 is estimated by doubling the mass flow of the transonic point to respect the strong peak in the fuel mass flow during ascent. For the initial design the consumed fuel mass for ascent is then estimated to 32.5 tons. Compared to 35.0 tons of the initial mission analysis it has to be remarked that the structural optimization was not considered in the initial mission analysis, so higher masses were used.

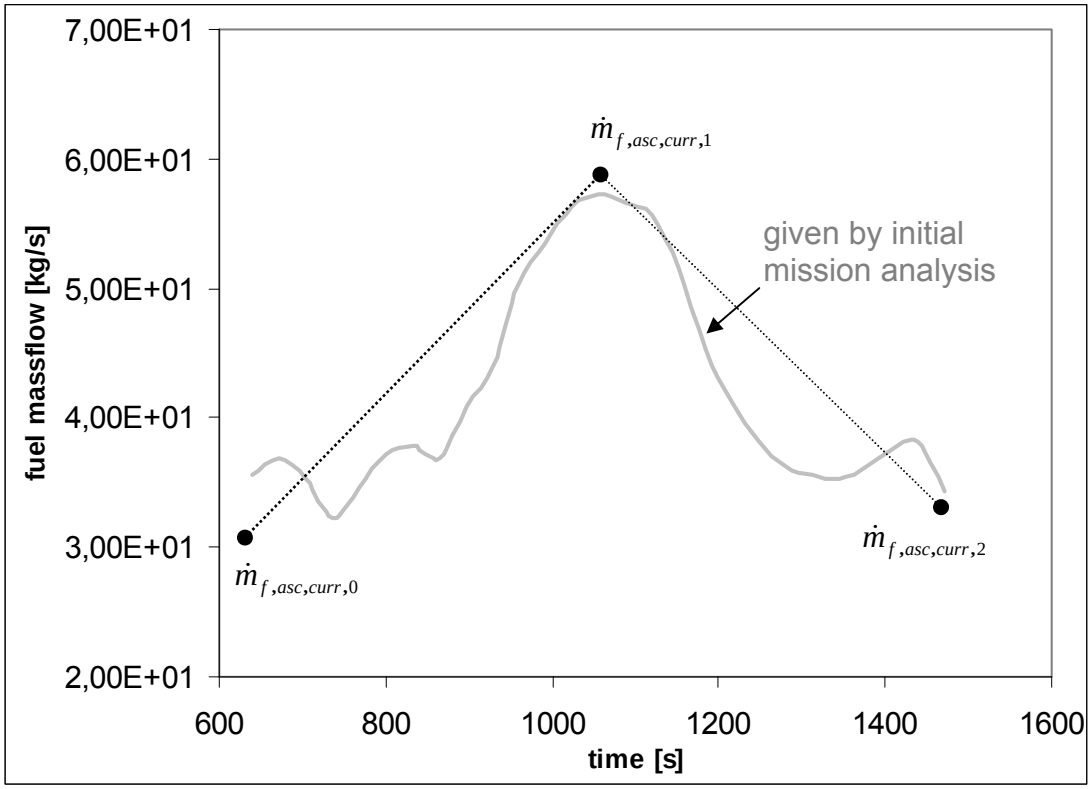

Fig. 3.12: Climb fuel mass flow over time – detailed analysis and 3-point approach

After the determination of the fuel mass for the accelerated climb the mass data for the cruise conditions is available. The BOC masses are defined:

$$m_{fuel,boc} = m_{fuel,\mathbf{max}} - 0.05 \cdot m_{gtow} - m_{fuel,ascent} \tag{3.11}$$

$$m_{boc} = m_{oe} + m_{fuel,boc} \tag{3.12}$$

Finally the EOC masses are defined by considering a reserve of 5 % of the BOC fuel mass:

$$m_{fuel,eoc} = 0.05 \cdot m_{fuel,boc} \tag{3.13}$$

$$m_{eoc} = m_{oe} + m_{fuel,eoc} \tag{3.14}$$

With this mass data the cruise CFD calculations can be performed. The Breguet range equation requires a constant lift coefficient. Hence the targeted lift coefficient is calculated by the BOC mass and equal in BOC and EOC CFD conditions. The only difference of both cruise cases is the

different horizontal stabilizer deflection. The deflection is influenced by the available fuel mass. The BOC fuel mass results in a COG range of about 7 m after the method described in chapter 3.2. To trim the configuration a deflection of 3° is needed. With increasing fuel mass consumption the COG range reduces and the deflection has to change to 7° to still fulfil trim conditions. At the same time the angle of attack has to be reduced for constant lift flight. Although the angle of attack is reduced the configuration drag is slightly higher due to the higher horizontal stabilizer drag. Thus the lift to drag ratio at end of cruise is lower compared to the begin of cruise lift to drag ratio. During the cruise the configuration have to climb due to the constant lift coefficient. The increase in altitude can be estimated to about 900 m for the initial configuration. However there is no direct impact on the cruise range but the descent range should be altered. At the moment no feasible descent model exists in the MDO process to consider climbing cruise effects on the configuration performance.

Two different throttle cases are considered for both cruise points resulting in four CFD calculations. All four cases can be run in parallel because there are no dependencies. With the aerodynamic analyses the final database of the current configuration is complete. Post-processing of the database updates all global constraints which are not part of a certain MDA module and finally the objective function based on the Breguet cruise range. The objective function combines all the mass, engine, aerodynamic and flight mechanic data which were collected during the performance of the MDA chain. The MDA chain is finished by sending the objective function value to the optimizer environment.

3.6 Design parameters

Due to the parameterized geometry model a huge set of design parameters is available. But as one of the main drivers for the overall MDO time the number of design parameters has to be restricted. A set of design parameters is chosen which mainly influences:

- Fuselage cross section on forebody
- Nose position
- Forebody and tail thickness
- Main wing position and size
- Horizontal stabilizer size and deflection angles depending on mission point
- Nozzle design

Figure 3.13 shows all design parameters. To reduce overall time the nozzle parameters change only the cruise state. Hence re-meshing of the transonic nozzle zone is not needed. The initial value for every design parameter is taken of the HYCAT 1A reference and listed in Table 3.8. The parameterization works with absolute and relative values. For the latter the references are listed in the last column of the table. There are two important references, the fuselage height and half width at cabin sections which are constant and they are defined by:

$$t\_Fuselage = 5.79\text{m}$$

$$b\_Fuselage = 4.47\text{m}$$

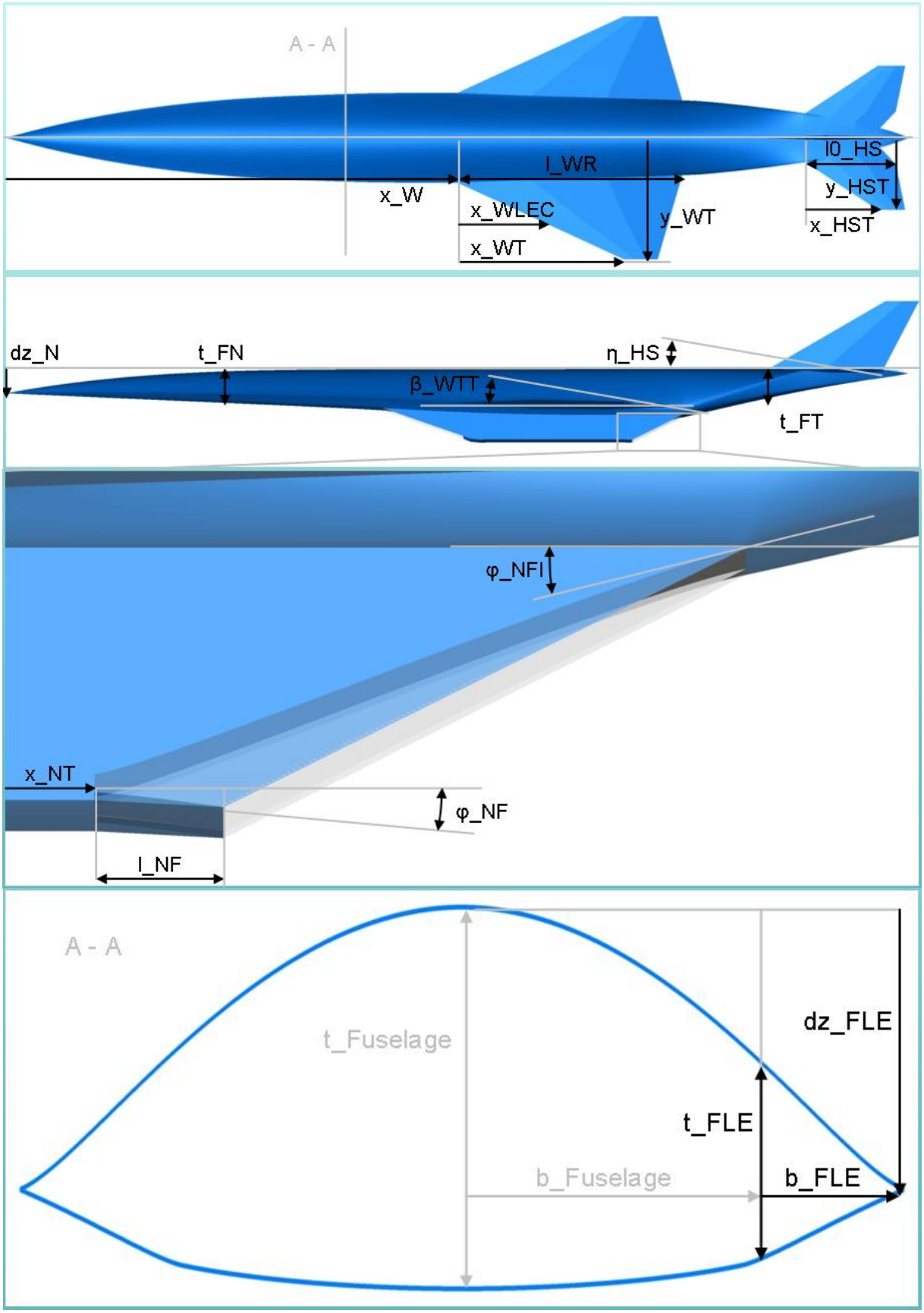

Fig. 3.13: Design parameters

Parameter	Initial value	Unit	Reference
dz_Nose	50.0	%	t_Fuselage
t_FuselageNose	60.0	%	t_Fuselage
t_FuselageTail	40.0	%	t_Fuselage
b_FuselageLeadingEdge	20.0	%	b_Fuselage
t_FuselageLeadingEdge	18.0	%	t_Fuselage
dz_FuselageLeadingEdge	80.0	%	t_Fuselage
x_Wing	54.0	m	-
x_WingTip	20.0	m	-
l_WingRoot	27.0	m	-
l0_WingProfile	33.0	%	Profile root length
x_WingLeadingEdgeCrank	50.0	%	x_WingTip
y_WingTip	14.56	m	-
ß_WingTipTwist	1.0	°	-
l0_HS	10.5	m	-
x_HSTip	8.7	m	-
y_HSTip	5.7	m	-
η_HSTransonic	1.5	°	-
η_HSBeginOfCruise	3.0	°	-
η_HSEndOfCruise	6.5	°	-
x_NozzleThroat	73.5	m	-
l_NozzleFlap	1.5	m	-
φ_NozzleFlap	5.0	°	-
φ_NozzleFuselageInterface	12.0	°	-

Table 3.8: Initial design parameter set

3.7 Objective function and global constraints

The objective function includes the ratio between the Breguet range of the current configuration and a reference range. For the reference range the Breguet range of the initial configuration is chosen and is determined to 3089 km. By normalizing the range it is simpler to integrate configuration constraints described by penalty functions. The Breguet range definition and final formulation of the objective function are:

$$R_B = \frac{v_{cr}}{sfc_{cr}} \cdot \frac{L}{D}\bigg|_{cr} \cdot \ln \frac{m_{boc}}{m_{eoc}} \tag{3.15}$$

$$OF = \frac{R_{B,curr}}{R_{ref}} \cdot \frac{1}{p} \tag{3.16}$$

With:

$$p = 1.0 + \sum p_i \tag{3.17}$$

Where as:

OF	Objective function
$R_{B,curr}$	Breguet range of current configuration
R_{ref}	Reference range
p	Penalty function
p_i	Penalty function of constraint *i*

The appearance of the penalty functions is shown in Figure 3.14. Hence for every constraint a slope, a minimum and a maximum allowable value have to be defined. The slope value describes the influence of the constraint to the objective function whenever it is violated.

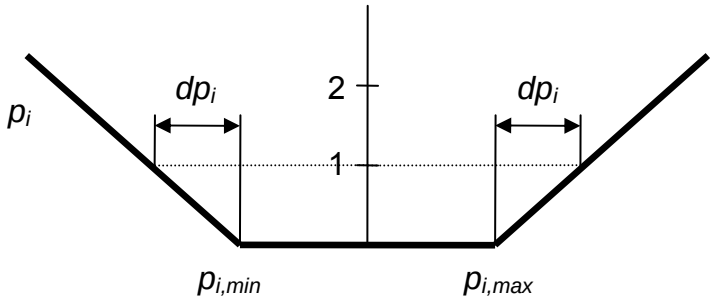

Fig. 3.14: Penalty function

The global constraints of the Mach 6 SST are summarized in Table 3.9. They include structural parameters, cruise intake air mass flow and trim checks by comparing centre of pressure with centre of gravity for several mission states. Further constraints like targeted lift for steady horizontal flight simulations are integrated in the corresponding modules. An exception occurs for the two structural constraints, the first eigen-frequency and the maximum “von Mises” stress. Both are already included in the structural optimization procedure. Due to the internal optimization strategy of the NASTRAN solver slight violation of the two constraints are accepted to find a feasible solution. Hence to match the global requirements both constraints are additionally checked here a second time.

constraint		p_min	p_max	dp
f_1stMode	Hz	2.5	-	0.5
δ_max,vonMises	MPa	-	400	50
mp_air_cruise	kg/s	1590	1750	100
m_glow	kg	-	300000	5000
x_cop_ts	m	x_cog_min*	x_cog_max*	5
x_cop_boc	m	x_cog_min*	x_cog_max*	1
x_cop_eoc	m	x_cog_min*	x_cog_max*	1

*special for every configuration

Table 3.9: Global constraints

4 MDO runs

4.1 Overview of the performed MDO runs

During the ATLLAS project three complete MDO runs were performed. With every MDO run the MDO tool was extended by improving the level of detail and accuracy. The first run was dominated by aerodynamic CFD analysis. The engine “black box” model was already integrated. Structural layout was not considered and configuration masses were only determined by geometrical values. Furthermore only the begin of cruise point was covered. Figure 4.1 shows the final configuration of the first run. In this case the cruise range was improved by 10 % mainly induced by the lift to drag improvement of 9%. The major changes are the wing and the horizontal stabilizer size and position.

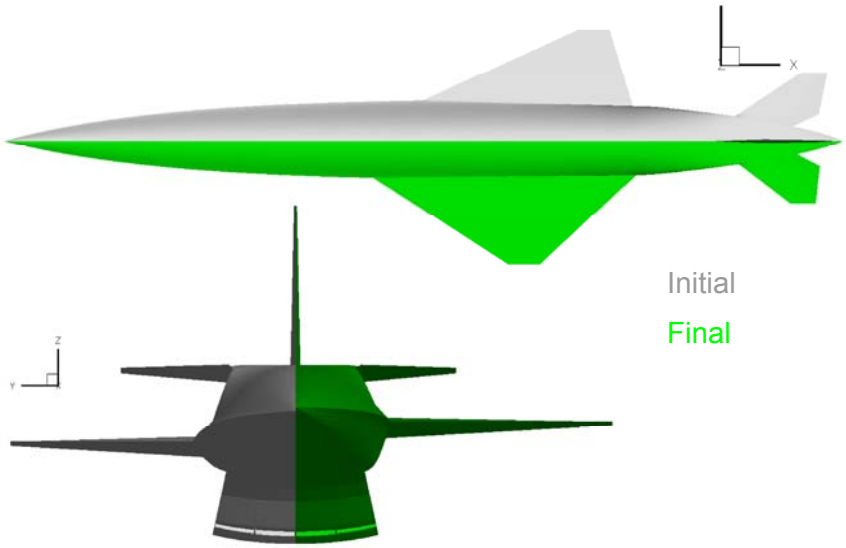

Fig. 4.1: Initial and final configuration of the cruise MDO run

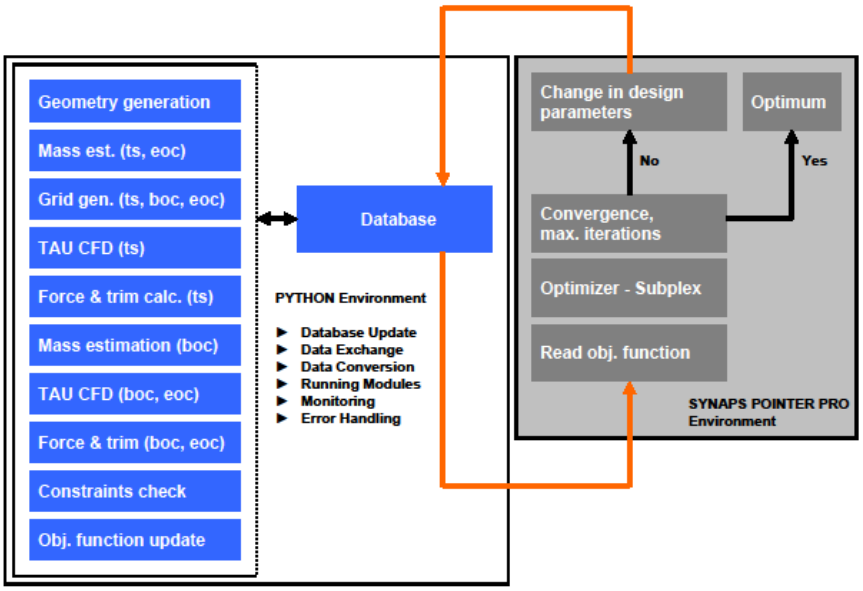

Fig. 4.2: Intermediate state of the MDO process

After the initial MDO run the process was extended by the multiple mission point integration. Thus the second cruise point at end of cruise and the transonic mission point at Mach number 1.3 were included. Although the mass analysis was improved, FEM modelling and analyses were still not implemented. At this stage the modular setup of the MDO process was advanced. However the complexity and computational costs of the MDO process increased strongly. Hence the major objective of the second MDO run was the inspection of the functionality and the interaction of the several MDO modules like it is shown in Figure 4.2. Figure 4.3 contains the objective function characteristics and some chosen configurations during the MDO process.

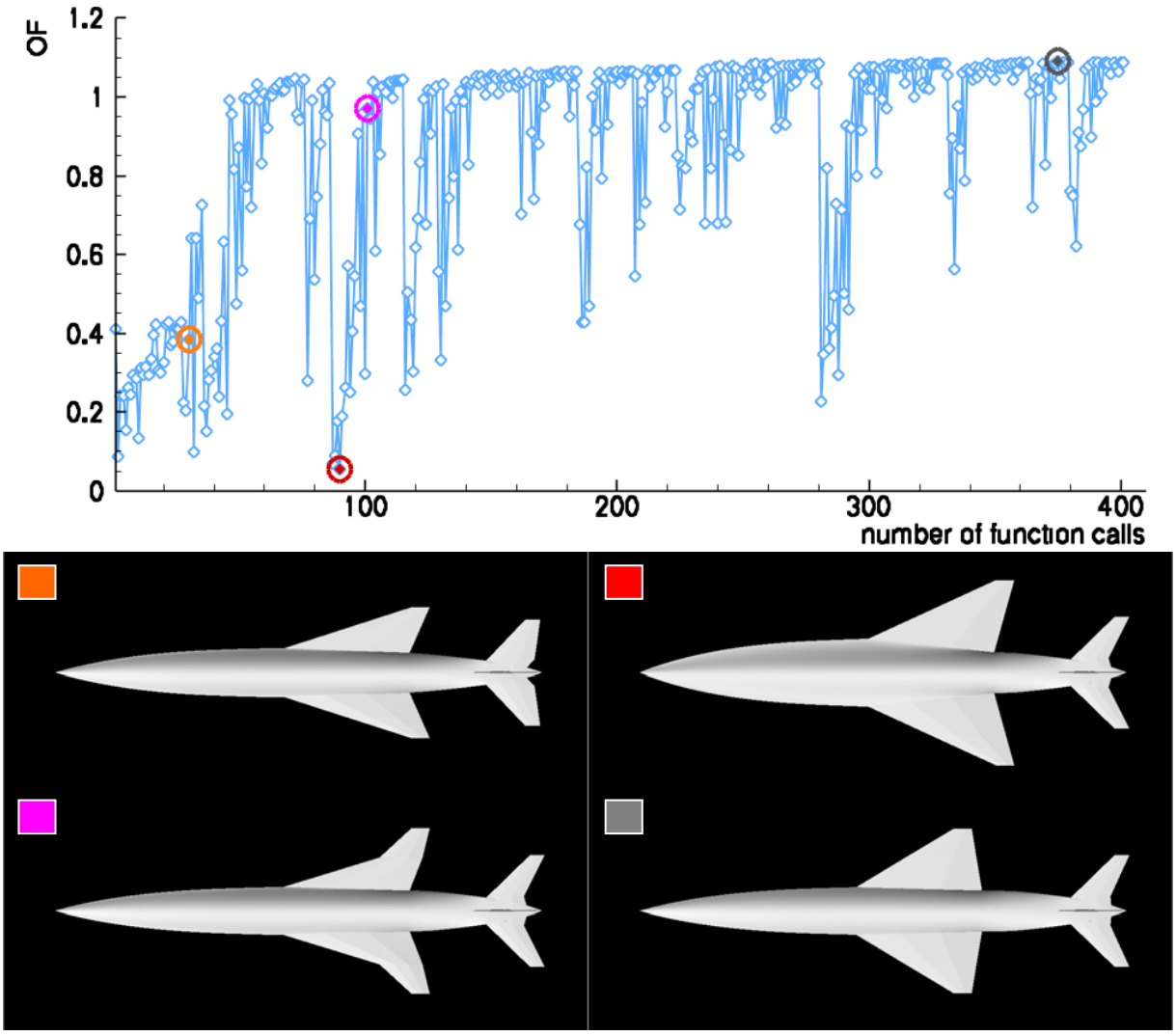

Fig. 4.3: Objective function characteristics and different configurations of the second MDO run

With the second MDO run the functionality of the several modules could be shown. Consequently the task for the final MDO process can be formulated. This includes the implementation of the engine model of ONERA, the FEM module based on the FOI input and improvement of the force analysis by including an interpolation strategy. The setup and the application of the final MDO process is presented here and in reference [3]. The characteristics and results of the final MDO are discussed more in detail in the following chapters.

4.2 Objective function characteristics of the final 3-point MDO run

The characteristics of the objective function in addition with some configuration examples are demonstrated in Figure 4.4. The reference range in the objective function [3.16] is the initial cruise range of 3098 km. A noisy behaviour of the objective function can be seen. This is due to the constraints penalty function which reduces the objective function whenever at least one constraint is violated. Hence for every lower peak it is pretty sure that a constraint violation occurred. Furthermore the objective function characteristics can be divided into three sections separated after about 140 and 280 iterations where always a strong increasing of the objective function can be observed. The stepwise increase is working along with the evaluation of the SUBPLEX cycles of the optimizer strategy described in [3]. In every cycle the design parameters are arranged in sub-spaces consisting of 2-5 parameters. After every cycle the optimum of the current arrangement of the design parameter sub-spaces is found. Depending on the influence on the objective function the design parameters are then rearranged hence with increasing number of cycles the sub-spaces contain design parameter groups of similar influence level.

The MDO run is stopped after 520 iterations. Due to the experience of former MDO runs, which were performed in the ATLLAS project, no arbitrative improvement is expected. Further changes are only affecting the appearance respectively reduction of the constraint violations. Due to number of constraints the optimum is in generally found at the lower or upper bound of one or more constraints. Hence also with small changes in the design parameters the objective function is switching between constraint violations or not. To smooth this effect the penalty functions have a user defined slope outside the bound instead of using a jump function at the bounds, see also Figure 3.14. Additional with every new cycle of the SUBPLEX optimizer the magnitudes of design parameter modifications get smaller leading to fewer changes in the objective function over the time.

The complete time needed for a single iteration is between 3 and 5 hours. The time differences between different iterations are mainly due to unpredictable queuing time of the used cluster systems. Against that the neat analysis time is very similar. At the end the overall time of the entire MDO process is 3 month.

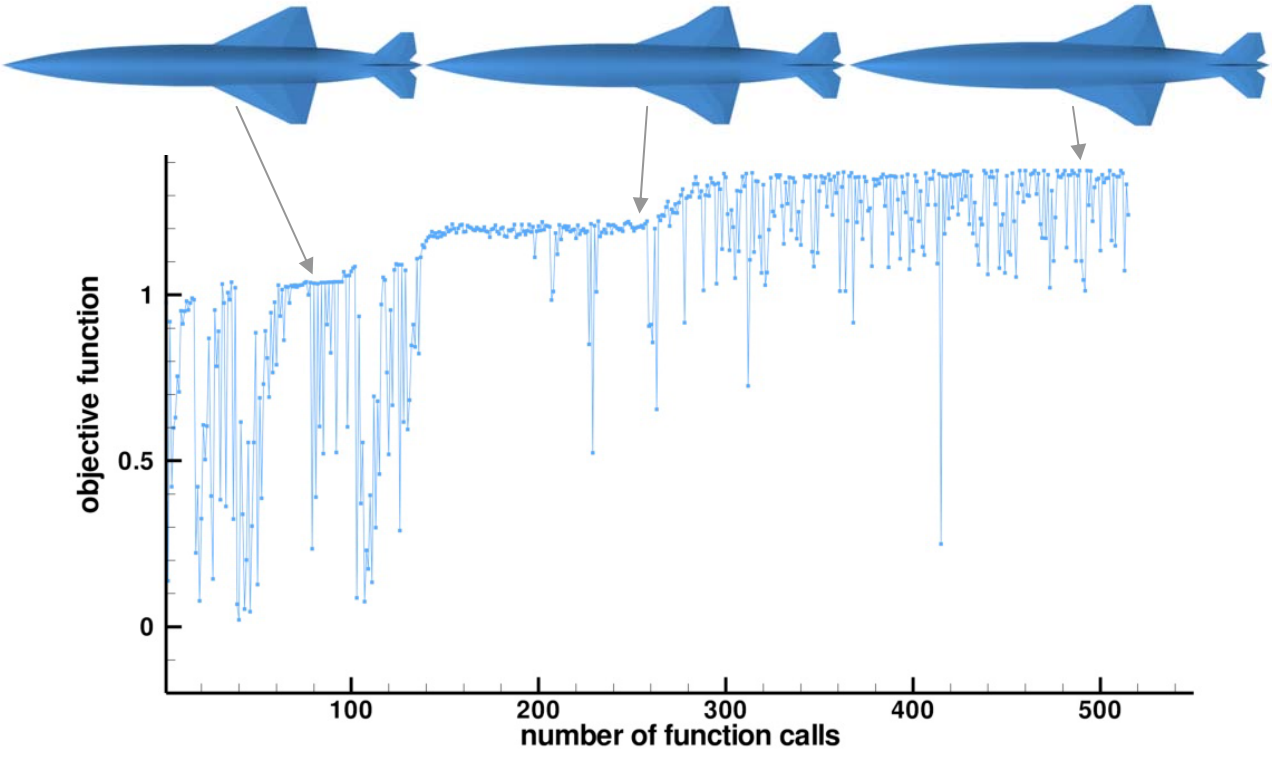

Fig. 4.4: Characteristics of objective function

4.3 Discussion of the results of the final 3-point MDO run

As demonstrated in Figure 4.4 during the optimization the objective function is increased from 0.97 to 1.38. This means starting from a slightly penalized configuration the final configurations objective function is improved by almost 40%. Figure 4.5 shows several views of the initial and the final configuration. At first the visual changes of the configuration seem less then expected. The most obvious changes are the enlarging of the forebody, modifications of the wing and the horizontal stabilizer geometry as well as the nozzle design. These changes are comprehended by comparing the design parameters which are presented in Table 4.1. It is shown that there are also changes in the wing span width and wing vertical position given by the forebody leading edge z-component. Additionally the double-trapezium wing profile is strongly modified by moving the middle edges to each other. It seems the profile shape is tending to a diamond profile. Against that there are only marginal displacements of the nose and the wing tip position as well as a very small increase in tail thickness. To discuss the improvement of the objective function further configuration properties have to be taken into account.

During the MDO process for every configuration a database is created containing more then 300 parameters to describe aerodynamic, propulsion, structural and mission performance. For clearance Table 4.2 summarizes some chosen properties of the initial and final configuration. In the Table the forces and engine parameters for begin of cruise and end of cruise conditions are listed. For BOC conditions additionally the lift components of several configuration parts are included to show the changes in lift production. At the end of Table 4.2 several important mass data is given.

The table indicates that a major improvement results on the changes in structural composition. By increasing the overall weight by 5 tons at the same time the fuel weight is increased by 10 tons. Compared to the initial configuration it produces a much better weight ratio which is an important part of the Breguet range equation (3.15). In contrast the increase in the fuel consumption during the accelerating climb phase due to the higher weight is relatively small and hence it has only a minor effect on the overall performance. The increased fuel mass is produced by enlargements of the tank volumes especially the bow tank. All parameters influencing the forebody cross section shape are extended resulting in a higher tank volume. At the same time the structural weight is reduced by 6 %.

The second point is the obviously decrease of the specific fuel consumption also seen as lower throttle level and fuel mass flow. There is a small drag reduction in the intake, probably due to the forebody and angle of attack modifications. But mainly it is caused to changes in the nozzle design especially length and deflection of the nozzle flap. On the one hand this is leading to a higher nozzle thrust Fx. On the other hand the lift production of the initial nozzle is reversed to a down force. In the overall lift balance it is compensated by the other components like fuselage, wing and horizontal stabilizer. For example the lift produced by the horizontal stabilizer in BOC conditions is increased by over 30 %. Although the projected surface area of the horizontal stabilizer and the deflection angle are only slightly increased the impact on the local lift is very strong. At the same time the angle of attack is altered to match the targeted lift condition and the trim capabilities are maintained. It has to be mentioned that a direct comparison of the forces is not necessarily meaningful due to primary differences like the targeted lift. These are difficulties of the interaction of several parameters in a multidisciplinary environment and finally the reason that for instance as objective function the range is chosen and not single forces. For similar reasons and in addition with the influence of the hypersonic integrated propulsion system following considerations are explained. Table 4.2 contains the force values based on the force definition described in [3] by adding several configuration surface components to certain groups e.g. main wall, intake etc. Afterwards the group force is composed by the pressure distribution of the containing surfaces. At a first view it seems that there is no change in the lift to drag ratio and only an improvement in the specific fuel consumption is observed. But the question remains what is drag and what is thrust? In Figure 4.6 the pressure distribution on the lower side for the initial and the final configuration is

plotted. The black line indicates approximately the end of the nozzle force group which is due to the definition constant in x-position. Behind the x-position the pressure force is counted into the main wall group. As you can see the nozzle expansion is extended backwards in the final design. Thus more fraction of the expansion is added to the main wall group. In the defined force analysis this results in a better nozzle thrust whereas the drag of the main wall remains almost constant and hence there is no improvement in the lift to drag ratio. Using alternative force balance approaches, for example by defining the end of the nozzle group by a certain pressure or adding the complete lower tail surface to the nozzle group, this behaviour is changed. Then the nozzle thrust can show minor changes and the main wall drag is reduced indicating a better lift to drag ratio and the same specific fuel consumption. But this definition has no influence on the overall performance. Finally the range equation contains both parts which can be described by the factor f_{api} merging the aerodynamic and propulsion performance:

$$f_{api} = \frac{1}{sfc} \cdot \frac{L}{D} \tag{4.1}$$

With the specific fuel consumption given by:

$$sfc = \frac{\dot{m}_{fuel} \cdot g}{T} \tag{4.2}$$

By replacing sfc in equation (3.15) and assuming constant lift during cruise it is shown that the cruise range is only depending on the masses and the needed fuel mass flow for steady horizontal flight. The last point is very important due to the equations are only valid if:

$$L = W \tag{4.3}$$

$$T = D \tag{4.4}$$

The cruise range is:

$$R_B \approx \frac{v_{cr} \cdot m_{boc}}{\dot{m}_{fuel}} \cdot \ln \frac{m_{boc}}{m_{eoc}} \tag{4.5}$$

At the moment the MDO tool uses equation (3.15). But it seems equation (4.5) defines the problem in a better way due to all involved parameters are not depending on further definitions. This aspect will be considered in future. However the steady horizontal flight conditions have to be fulfilled and they are respected during the MDA process. When using (3.15) the forces are a question of definition and as mentioned above a direct comparison can mislead. If equations (3.3) and (4.4) are true then whenever defining for instance the drag component immediately the thrust component is determined. The magnitude is less important, but influences derived values like the lift to drag ratio. For the lift and the weight the definition is easier but as demonstrated for thrust and drag different approaches can be used. The “black box” engine model and the multidisciplinary analysis demonstrates that for the ATLLAS Mach 6 SST based on an integrated propulsion system no separation of the propulsion system and the aerodynamic performance have to be done. Hence

it is recommended using the aerodynamic-propulsion interaction factor f_{api} when comparing different configurations. As already mentioned for this reason the cruise range is chosen for the objective function.

In Table 4.2 it is demonstrated that the aerodynamic-propulsion interaction is improved by 16 %. In addition with the strong improvement of the weight ratio the result of the final 3-point MDO process can be explained. A similar discussion of the aerodynamic-propulsion interaction can be found in [9] wherein the configuration performance is expressed as range factor and cruise efficiency. By multiplying (4.1) with the cruise velocity gives the range factor. Both, range factor and cruise efficiency can be found in Table 4.2 for the initial and final configuration.

Parameter	Unit	Initial value	Final value
dz_Nose	%	50.0	50.6
t_FuselageNose	%	60.0	78.4
t_FuselageTail	%	40.0	41.6
b_FuselageLeadingEdge	%	20.0	34.5
t_FuselageLeadingEdge	%	18.0	25.7
dz_FuselageLeadingEdge	%	80.0	70.9
x_Wing	m	54.0	53.44
x_WingTip	m	20.0	20.16
l_WingRoot	m	27.0	28.02
l0_WingProfile	%	33.0	52.9
x_WingLeadingEdgeCrank	%	50.0	62.5
y_WingTip	m	14.56	15.63
ß_WingTipTwist	°	1.0	2.04
l0_HS	m	10.5	11.07
x_HSTip	m	8.7	6.83
y_HSTip	m	5.7	5.58
η_HSTransonic	°	1.5	2.43
η_HSBeginOfCruise	°	3.0	3.71
η_HSEndOfCruise	°	6.5	5.27
x_NozzleThroat	m	73.5	73.10
l_NozzleFlap	m	1.5	3.44
φ_NozzleFlap	°	5.0	0.05
φ_NozzleFuselageInterface	°	12.0	7.63

Table 4.1: Comparison of the initial and final design parameter set

Configuration 001 - initial

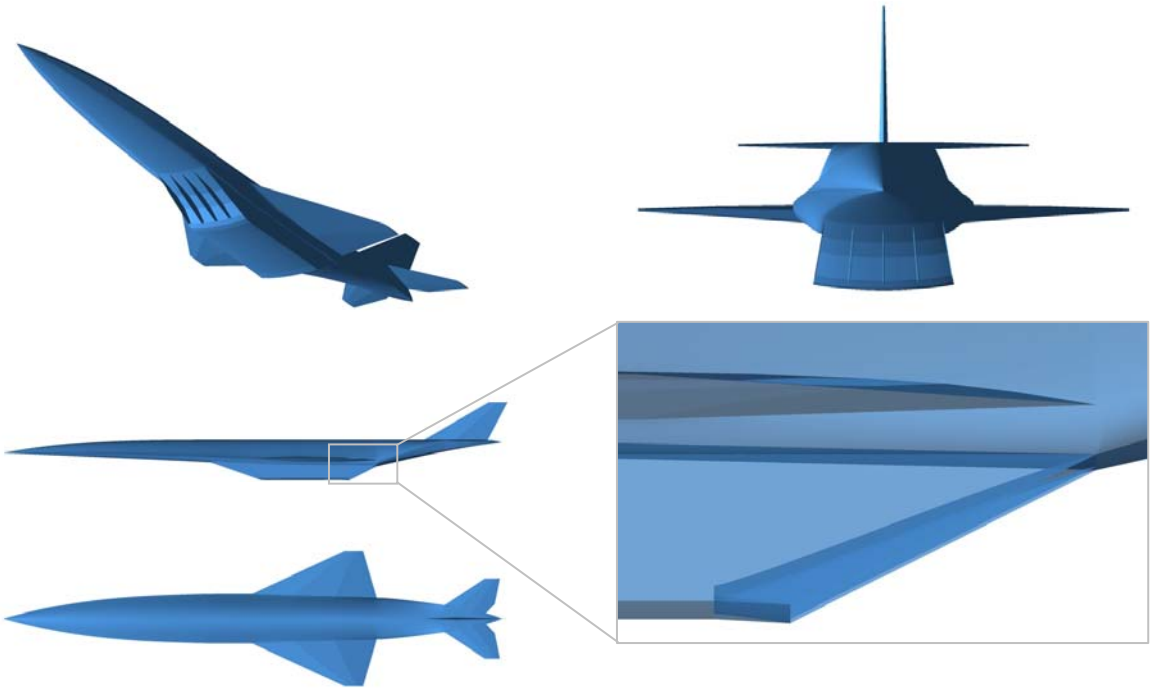

Configuration 493 - final

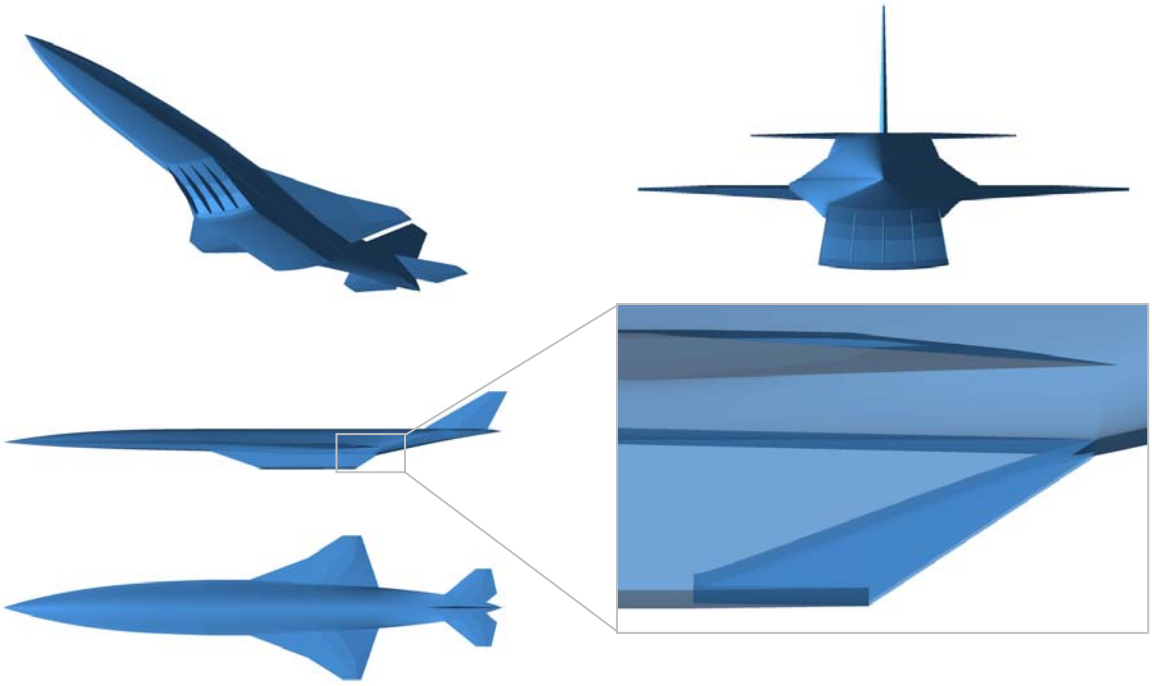

Fig. 4.5: Comparison of initial and final configuration

Parameter	*Unit*	*Configuration 001*	*Configuration 493*	*%*
Objective function	**-**	**0.98**	**1.38**	**40.8**
All constraints fulfilled	**-**	**false**	**true**	
R_Breguet	**km**	**3089.00**	**4250.00**	**37.6**
Fx_intake_boc*	N	663700.00	641100.00	-3.4
Fz_intake_boc*	N	-11100.00	34500.00	-410.8
Fx_nozzle_boc	N	-714800.00	-756000.00	5.8
Fz_nozzle_boc	N	145800.00	-187500.00	-228.6
Fx_cc_boc	N	-337500.00	-290900.00	-13.8
Fz_cc_boc	N	17400.00	16100.00	-7.5
mp_fuel_boc	kg/s	31.20	27.90	-10.6
Throttle_boc	%	53.50	45.50	-15.0
sfc_boc	1/s	7.85E-04	6.71E-04	-14.5
D_boc	N	387400.00	404600.00	4.4
L_boc	N	2144300.00	2219600.00	3.5
L_fuselage_boc	N	1033200.00	1238400.00	19.9
L_wing_boc	N	723100.00	807900.00	11.7
L_hs_boc	N	238000.00	313900.00	31.9
L/D_boc	-	5.53	5.48	-0.9
alpha_boc	°	2.93	3.14	7.2
x_cop_boc	m	58.10	59.10	1.7
Fx_intake_eoc*	N	653100.00	635900.00	-2.6
Fz_intake_eoc*	N	-20200.00	29800.00	-247.5
Fx_nozzle_eoc	N	-715200.00	-754600.00	5.5
Fz_nozzle_eoc	N	143000.00	-190400.00	-233.1
Fx_cc_eoc	N	-340800.00	-293100.00	-14.0
Fz_cc_eoc	N	15800.00	15600.00	-1.3
mp_fuel_boc	kg/s	31.50	28.10	-10.8
Throttle_eoc	%	54.10	45.90	-15.2
sfc_eoc	1/s	7.61E-04	6.64E-04	-12.7
D_eoc	N	403000.00	411800.00	2.2
L_eoc	N	2136800.00	2215400.00	3.7
L/D_eoc	-	5.30	5.38	1.5
alpha_eoc	°	2.64	3.01	14.0
x_cop_eoc	m	61.30	60.70	-1.0
sfc_m	**1/s**	**0.00**	**0.00**	**-13.7**
L/D_m	**-**	**5.42**	**5.43**	**0.2**
L/D/sfc_m	**s**	**7012.00**	**8141.00**	**16.1**
Rf	nm	6815.00	7912.00	16.1
eta_cr	-	1.02	1.19	16.1
m_gtow	kg	272000.00	277000.00	1.8
m_structure	kg	86400.00	81300.00	-5.9
m_fuel_max	kg	99800.00	109900.00	10.1
m_fuel_ascent	kg	45600.00	46300.00	1.5
ln(m_boc/m_eoc)	**-**	**0.24**	**0.29**	**20.8**

All forces in aerodynamic coordinate system (x – drag, z – lift)
* incl. intake corrections [3]

Table 4.2: Comparison of initial and final configuration properties

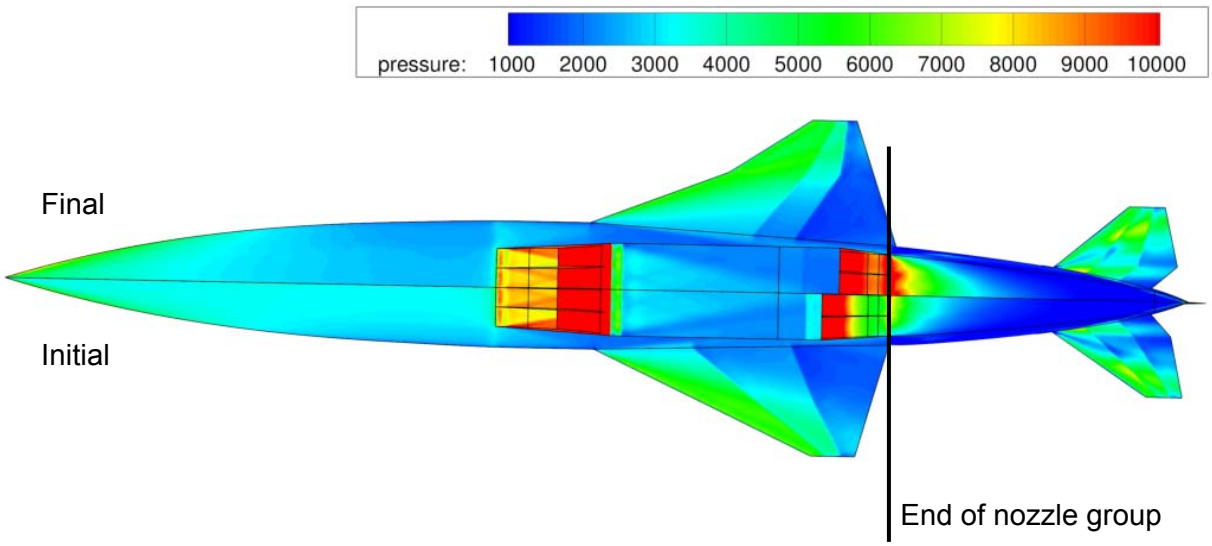

Fig. 4.6: Pressure distribution on lower configuration side (M = 6.0, throttle level = 60%)

4.4 Final comments on the Mach 6 design and the MDO process

The result of a final cruise range of 4250 km is still low. Respecting the considered reserve fuel and taking also the initial mission profile into account the maximum mission range of the final configuration can be roughly estimated to about 7400 km compared to 6200 km of the initial configuration. The estimation is based on 1200 km for the accelerated climb, 1500 km for the descent and 500 km due to reserve fuel. However the HYCAT 1A estimations of 9000 km mission range can not be confirmed within this work.

Table 4.3 extends the performance table given in [9] by the initial and the final ATLLAS Mach 6 configuration. The aerodynamic-propulsion interaction performance, expressed by the range factor, of the final ATLLAS Mach 6 configuration is above of the Concorde and the XB-70. Due to the use of hydrogen the cruise efficiency is significantly lower.

Aircraft	777-300ER	767-400ER	Concorde	XB-70	SR-71	HSR-TC	AM6-Init	AM6-Final
GTOW, Mg	351	204	185	246	63	342	272	277
OEW, Mg	168	103	80	115	27	147	152	147
Max. Fuel, Mg	200	73	95	137	36	167	100	110
Range fac., nm	16243	14409	7119	6158	5000	10378	6815	7912
Cruise eff.	6.9	6.1	3.0	2.6	2.1	4.3	1.0	1.2

Table 4.3: Weights, range factor and cruise efficiency (extension to [9])

Even after the MDO process a major disadvantage of the ATLLAS Mach 6 SST is the weak fuel mass to total mass fraction of 0.4. This is similar to subsonic aircrafts like the A380. For the Concorde for instance the mass ratio is 0.5. Hypersonic aircrafts have to raise this mass ratio due to they are in generally already penalized with lower lift to drag ratios respectively lower aerodynamic-propulsion performance. On the other hand the classical design of the configuration shows very good trim capabilities. Also the horizontal tail produces additional lift. Furthermore due to the compact wings structural stresses and strains due to pressure are assumed to be less

critical especially in cruise conditions. The wing volumes are not needed for fuel storage. Hence there is space left for sufficient wing and wing-fuselage interface design. In contrast due to the fuselage dimensions and non-cylindrical fuselage shape dynamic behaviour is an important issue.

The developed MDO process shows the capability to identify and take advantage of possible space for local improvements to raise a global configuration property like the cruise range. But due to complexity and the computational effort to manage and solve the problem, at the moment the entire MDO process has to be constrained at multiple places. Thus a complete redesign of the given configuration is not possible and principal initial design choices are maintained during the MDO process. The current MDO process couples important analysis methods of existing high-fidelity methods for the application of hypersonic aircrafts. It does not claim the fact to design a complete new configuration. It is thought to support and improve an existing baseline design. With further work on the MDO tool it is expected that in future more and more of the process constraints can be loosed also leading to global modifications of a given configuration.

Finally the major results of the MDO process are outlined:

- Successful coupling of CFD, FEM, multiple mission point analysis, propulsion integration and trim capability determination in one multidisciplinary analysis tool
- MDO process linkage to massive parallel computing system
- MDO process application on the ATLLAS Mach 6 SST
- Successful demonstration of the functionality and capability of the MDO process
- MDO process can start from a penalized system
- Cruise range improvement of 38%, from 3090 km to 4250 km
- Estimated entire mission range improvement of 25%, from 6200 km to 7400 km
- Major influence due to improvement in structural design and mass ratio
- Improvement in aerodynamic-propulsion interaction performance
- Final cruise range still low due general design influences

Conclusions

The application of the MDO process which was developed during the ATLLAS project is presented. The specific content and a detailed description of setup and requirements of the MDO process are given in the separate deliverable D2.4.1 [3]. In the presented work the main focus is the description of the application on the Mach 6 hypersonic configuration. The configuration is defined within the project and based on the HYCAT 1A configuration designed by Lockheed in the late 70's. Parameters of different physical disciplines e.g. propulsion, structure and mission were provided by different ATLLAS partners and serve as input for the MDO process. Thus a complete mass budget, a propulsion table, mission database and geometry parameters are available.

Within the ATLLAS project several MDO runs were performed whereas the last one includes all targeted disciplines. The former runs are shortly presented. In contrast the final MDO run is discussed in detail concerning objective function characteristics and MDO results. After the execution of the MDO process, which takes about 3 month in continuous computations, the objective function was increased by almost 40 %. The final cruise range of the ATLLAS Mach 6 SST is 4250 km. The relative huge improvement is explained by 1) the modification of the structural design and a better begin of cruise to end of cruise mass ratio and 2) an improved interaction between propulsion system and aerodynamic. It is demonstrated that the separation between the aerodynamic and propulsion can mislead the result interpretation. It is recommended to keep both aspects together due to overall performance is not influenced. This approach is supported due to the objective function is based on the Breguet range equation which contains the main aircraft forces lift, weight, drag and thrust. When simulating hypersonic cruise conditions including partial or full engine flow the classification of surface forces to drag or thrust is a question of definition. For a complete airframe-engine configuration in steady horizontal flight simulations the numerical computed "drag" coefficient have to be zero. Only then the entire configuration drag is compensated by the produced thrust. Thus classical aircraft parameters like the lift to drag ratio or the specific fuel consumption are depending on the used force definition and hence they are less suitable for comparison. The Breguet range formulation can be alternatively expressed as function of the fuel mass flow which seems more practical for hypersonic applications. The effort in the CFD analysis is needed to fulfil the constraints of lift is equal to weight and thrust is equal to drag.

For the presented MDO process on the Mach 6 SST several configuration constraints were introduced considering maximum respectively minimum values for important structural, mass, trim and propulsion parameters. The constraints are added to the objective function with a penalty function. This gives a flexible method for adding or removing further constraints.

Due to the results for future MDO processes the structural part of the MDO tool is one major point of interest in the future. The accuracy and the strategy for FEM-modelling and analysis including more load cases can be extended. Furthermore aeroelastic and thermodynamic effects could be included to both, the aerodynamic and the structural module. Hence possible future activities on the MDO tool are summarized by:

- Extensions inside existing modules:
  - Variants of static load cases, aeroelastic effects and improved constraints for the structural design
  - Extension and Improvement of the mission analysis including ascent and descent models

- Development of new modules:
  - Thermal prediction and influence on structure and aerodynamic performance
  - Sonic boom analysis

References

[1] G.D. Brewer, R.E. Morris, "*Hypersonic Cruise Aircraft Propulsion Integration Study Volume I/II*", NASA Contractor Report, CR-158926-1, 1979

[2] J.C. Ellison, "*Investigation of the Aerodynamic Characteristics of a Hypersonic Transport Model at Mach Numbers up to 6*", NASA Technical Note D-6191, 1971

[3] R. Dittrich, "*D2.4.1 Report on DLR MDO tool for high-speed design* ", ATLLAS, 2010

[4] R. Jarlas, H. Rabia, "*D2.4.7 Structural Design of Airframe*", ATLLAS, 2009

[5] "*TAU Technical Report*", DLR, Institute of Aerodynamics and Flow Technology, Braunschweig, Germany, 2007

[6] M. Weule, "*Aerothermodynamische Charakterisierung eines Hyperschalltransportflugzeuges* ", Diploma thesis, University of Technology, Braunschweig, Germany, 2008

[7] M. Kuhn, E. Klatt, S. Hackemann, "*D3.3.2 Part B – Test Samples and Test Report: CMC Material Characterization of C/C-SiC, OXIPOL and WHIPOX for Hot Vehicle Strcutures* ", ATLLAS, 2009

[8] A. Lang, M. Sippel, J. Klevanski, U. Atanassov, "*D2.4.3, D2.4.4, D2.4.5, D2.4.6, M6 propulsion data set, CAD model, mass estimation and trajectory analysis*", ATLLAS, 2010

[9] T. Cain, C. Walton, M. Zanchetta, "*D2.1.1 Cruise Efficiency*", ATLLAS, 2007